Please cite this article in press as: Kim et al., Skeletal muscle-on-a-chip in microgravity as a platform for regeneration modeling and drug screening, Stem Cell Reports (2024), https://doi.org/10.1016/j.stemcr.2024.06.010

Stem Cell Reports
Article
ISSCR
OPEN ACCESS

Skeletal muscle-on-a-chip in microgravity as a platform for regeneration modeling and drug screening

Soochi Kim,[1,6,7] Bugra Ayan,[2,7] Mahdis Shayan,[2,7] Thomas A. Rando,[1,3,8,*] and Ngan F. Huang[2,3,4,5,9,*]
[1]Department of Neurology and Neurological Sciences, Stanford University, Stanford, CA 94305, USA
[2]Department of Cardiothoracic Surgery, Stanford University, Stanford, CA 94305, USA
[3]Center for Tissue Regeneration, Repair and Restoration, Veterans Affairs Palo Alto, Health Care System, Palo Alto, CA 94304, USA
[4]Stanford Cardiovascular Institute, Stanford University, Stanford, CA 94305, USA
[5]Department of Chemical Engineering, Stanford University, Stanford, CA 94305, USA
[6]Present address: Department of Biotechnology and Bioinformatics, Korea University, Sejong 30019, Republic of Korea
[7]These authors contributed equally
[8]Present address: Eli and Edythe Broad Center of Regenerative Medicine and Stem Cell Research, University of California Los Angeles, Los Angeles, CA 90095 USA
[9]Lead contact
*Correspondence: trando@mednet.ucla.edu (T.A.R.), ngantina@stanford.edu (N.F.H.)
https://doi.org/10.1016/j.stemcr.2024.06.010

SUMMARY

Microgravity has been shown to lead to both muscle atrophy and impaired muscle regeneration. The purpose was to study the efficacy of microgravity to model impaired muscle regeneration in an engineered muscle platform and then to demonstrate the feasibility of performing drug screening in this model. Engineered human muscle was launched to the International Space Station National Laboratory, where the effect of microgravity exposure for 7 days was examined by transcriptomics and proteomics approaches. Gene set enrichment analysis of engineered muscle cultured in microgravity, compared to normal gravity conditions, highlighted a metabolic shift toward lipid and fatty acid metabolism, along with increased apoptotic gene expression. The addition of pro-regenerative drugs, insulin-like growth factor-1 (IGF-1) and a 15-hydroxyprostaglandin dehydrogenase inhibitor (15-PGDH-*i*), partially inhibited the effects of microgravity. In summary, microgravity mimics aspects of impaired myogenesis, and the addition of these drugs could partially inhibit the effects induced by microgravity.

INTRODUCTION

Representing approximately 40% of body weight, skeletal muscle is one of the most abundant tissues in the human body (Reid and Fielding, 2012). Skeletal muscle regenerates itself through satellite cells, a reservoir of quiescent muscle stem cells that can be activated with injury or disease and give rise to newly formed multi-nucleated myotubes and myofibers (Mauro, 1961; Morgan and Partridge, 2003). As civilian space travel to the International Space Station and beyond will become increasingly more common in the next century, it is important to better understand how microgravity affects the regenerative capacity of muscle. Mice exposed to microgravity have shown reduced muscle regeneration, compared to those in normal gravity, as demonstrated by relatively fewer postmitotic nuclei within myofibers as an indicator of impaired *de novo* muscle fiber formation (Radugina et al., 2018). Similarly, *in vitro* studies composed of murine myoblasts seeded within three-dimensional hydrogels in simulated microgravity also show reduced myogenesis, based on the formation of shorter and thinner myotubes with reduced fusion capacity (Ren et al., 2024). These data support a larger body of literature showing that microgravity exerts profound effects on skeletal muscle (Fitts et al., 2010; Juhl et al., 2021; Trappe, 2009).

The identification of countermeasures against the effects of microgravity on muscle regeneration is an increasing priority for continued space travel. Developing drugs that counteract the effects of microgravity is a promising strategy, but no Food and Drug Administration (FDA)-approved drug currently exists, partially due to the limited access of participants to microgravity conditions. In contrast, a muscle-on-a-chip in microgravity platform can be performed in a facile manner *in vitro* and can allow for screening many drugs in parallel. Through the US National Science Foundation and the Center for the Advancement of Science in Space (CASIS), we were offered a unique opportunity to perform tissue engineering and mechanobiology research aboard the International Space Station National Laboratory (ISSNL). With the assistance of astronauts, we applied our expertise in the engineering of skeletal muscle (Huang et al., 2006; Nakayama et al., 2019) toward the study of muscle myogenesis using a muscle-on-a-chip platform. By performing multi-omics analyses, we show that the muscle-on-a-chip platform in microgravity mimics salient aspects of impaired muscle regeneration after merely 7 days in microgravity. Furthermore, we demonstrate the feasibility of drug screening in this microgravity platform by using two drugs that partially prevent the negative effects of microgravity in the muscle-on-a-chip bioconstructs.

Please cite this article in press as: Kim et al., Skeletal muscle-on-a-chip in microgravity as a platform for regeneration modeling and drug screening, Stem Cell Reports (2024), https://doi.org/10.1016/j.stemcr.2024.06.010

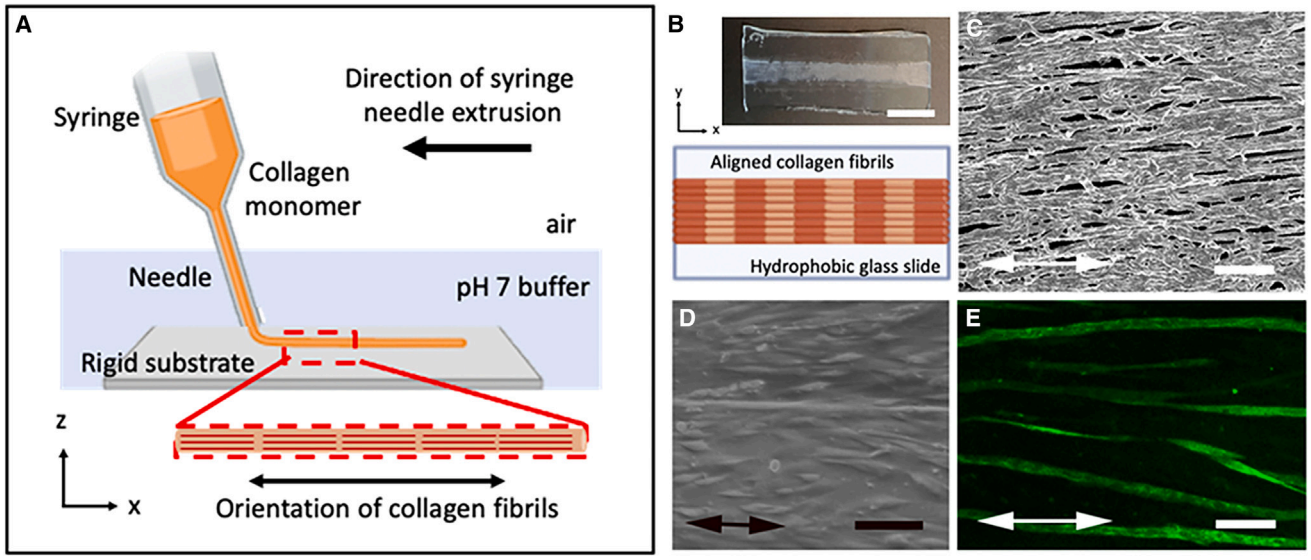

Figure 1. Generation and characterization of biomimetic skeletal muscle-on-a-chip platform

(A) Schematic depicting the fabrication of aligned collagen nanofibrils using shear-mediated extrusion of monomeric collagen into pH 7 buffer.

(B) Gross image and schematic of anisotropic collagen strips deposited onto hydrophobic glass chips.

(C) Scanning electron microscopy analysis shows highly organized anisotropic collagen fibrils.

(D) Seeding of primary human skeletal muscle cells shows cell alignment along the direction of the collagen nanofibrils (denoted by arrow).

(E) In induction media, the cells fuse to form parallel-aligned myotubes, as shown by myosin heavy-chain staining (green). Scale bars: (B) 5 mm, (C) 1 μm, (D–E) 100 μm.

RESULTS

Engineering of muscle-on-a-chip system in microgravity

To adapt engineered muscle for microgravity conditions aboard the ISSNL, we developed a muscle-on-a-chip platform to immobilize the engineered muscle onto rigid hydrophobic glass for culture within a flight-compatible custom-made bioreactor. Skeletal muscle constructs composed of primary human myotubes on parallel-aligned collagen nanofibrils were generated by a facile shear-based collagen extrusion assay. Taking advantage of collagen fibrillogenesis being controlled by both pH and shear, we sheared acidic monomeric collagen type I from a blunt needle onto a rigid glass substrate bathed in pH neutral buffer (Figure 1A), forming strips of collagen with highly organized nanofibrils. The collagen strips were composed of nanofibrils that were <100 nm in diameter, and the strips were then bundled together (Figures 1B and 1C). The anisotropic organization of the collagen fibrils provides topographical patterning cues to induce primary human skeletal muscle cells to organize along the direction of the nanofibrils (Figure 1D) and subsequently to form aligned myotubes (Figure 1E). The cell-seeded scaffolds were denoted as a "muscle-on-a-chip."

To adapt the muscle-on-a-chip platform to microgravity, microgravity-compatible bioreactors were custom-made by BioServe Space Technologies. Prior to launch, the flight hardware was assembled by securing the muscle-on-a-chip bioconstructs within the chamber, filling the chamber with medium, and sealing with an air-permeable membrane stabilized with a solid frame (Figures 2A, S1A, and S1B). During transit to the ISSNL on a Cygnus vehicle, the bioreactors were transported within gas-sealed space habitats that maintained temperature and CO_2 levels (Figures 2 and S1C). Upon arrival at the ISSNL, the space habitats housing the bioreactors were placed into the Space Automated Bioproduct Lab incubator and maintained at 37°C and 5% CO_2. The experiments were initiated (day 0) in microgravity with the syringe-mediated replacement of the media with induction media that supports myotube formation (Figure 2B). Comparable bioreactors were assembled on Earth in normal gravity conditions, and the same experiments were performed in parallel to samples in microgravity.

Microgravity alters myogenesis and genetic program in skeletal muscle-on-A-chip

We first quantified myotube formation from healthy donor-derived engineered muscle after 7 days of exposure to

Please cite this article in press as: Kim et al., Skeletal muscle-on-a-chip in microgravity as a platform for regeneration modeling and drug screening, Stem Cell Reports (2024), https://doi.org/10.1016/j.stemcr.2024.06.010

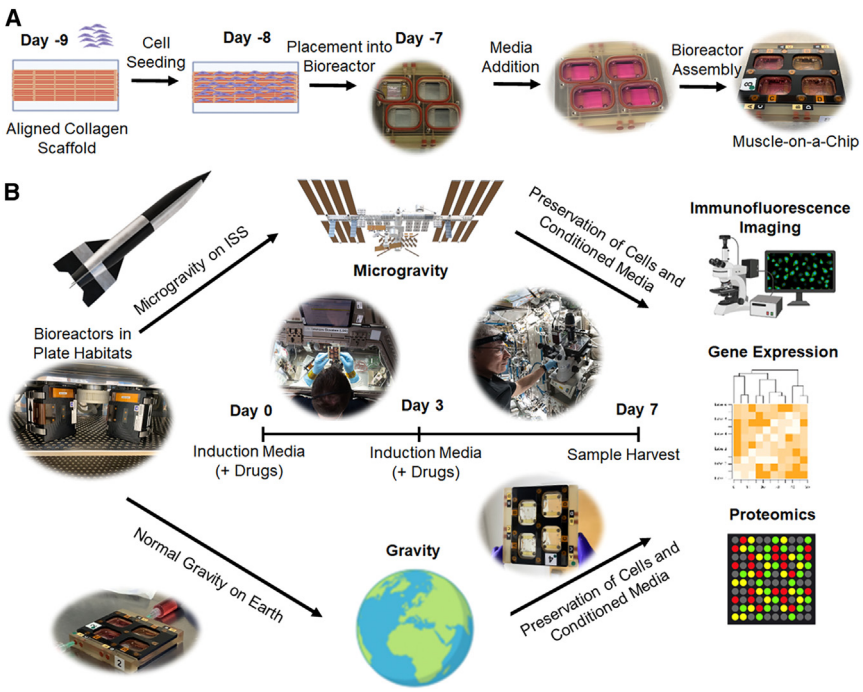

Figure 2. Preparation of muscle-on-a-chip devices for microgravity studies and experimental overview

(A) The overview of muscle-on-a-chip preparation consists of seeding human muscle cells onto immobilized aligned nanofibrillar collagen scaffolds followed by cell seeding. After one day, the cell-seeded scaffolds are placed into bioreactors and filled with growth media. The bioreactor is then secured with screws for transportation to the ISSNL.

(B) The experimental overview consists of incubating the bioreactor during transit to the ISSNL in plate habitats that provide temperature maintenance during transport to the ISSNL or in normal gravity conditions on Earth. Upon docking at the ISSNL, microgravity experiments began (day 0) with media change into an induction media that supports myotube formation. In some experiments, drugs were added to the media on day 0 and again on day 3. On day 7, the conditioned media were extracted, and the samples were stabilized in RNAlater or fixed in paraformaldehyde for analysis on by RNA sequencing, proteomics analysis, or myotube formation.

microgravity. Our results showed reduced myotube length, width, and fusion index in microgravity, compared to gravity (Figure S2; Table S1). This finding of reduced myogenesis in microgravity was then corroborated by transcriptional analysis. Following 7 days of differentiation and myotube formation, the muscle-on-a-chip bioconstructs in both microgravity and gravity from two healthy donors were assessed by RNA sequencing (RNA-seq). We detected 58,735 genes, of which 25,914 passed the threshold for expression. Transcripts of low count, expressed in less than two samples, were excluded. Samples were clustered by the gravity condition (Figure 3A), where 107 genes were upregulated and 286 genes were downregulated in microgravity samples with a false-discovery rate (FDR) < 10% (Figure 3B and Table S2). Database for Annotation, Visualization and Integrated Discovery (DAVID) analysis classified 104 upregulated genes in microgravity into the Cellular Component Gene Ontology (GO-CC) term. The analysis shows significant enrichment in genes encoding proteins located in various subcellular structures (Figure 3C). Among these genes, 14 of them were annotated under the "mitochondrion" GO-CC (Figure 3D). For example, mitochondrially encoded cytochrome *c* oxidase III (*MT-CO3*) has previously been reported to increase in muscle stem cells during aging (Perez et al., 2022), which is associated with impaired regeneration. Since muscle has high metabolic function, proper mitochondrial biogenesis is necessary for regeneration.

Pathway enrichment analysis also supported changes in metabolic pathways, including genes implicated in cholesterol, lipid, and fatty acid metabolism (Figure 3E). Among them, fatty acid desaturase 1 (*FADS1*) and mitochondrial matrix Lon peptidase 1 (*LONP1*) were also implicated in cellular responses to muscle regeneration (Huang et al., 2020). Additionally, the pro-apoptotic gene, Bcl-2 related ovarian killer (*BOK*), along with cell survival and differentiation-associated genes, serum/glucocorticoid regulated kinase 1 (*SGK1*) and NADPH oxidase 4 (*NOX4*) (Dehner et al., 2008; Pedruzzi et al., 2004; Yakovlev et al., 2004), was upregulated in microgravity. *SGK1* and *NOX4* are associated with muscle mass maintenance and myoblast differentiation, respectively (Andres-Mateos et al., 2013; Youm et al., 2019). In particular, *SGK1* regulates muscle homeostasis by the downregulation of proteolysis and autophagy (Andres-Mateos et al., 2013). *NOX4*-derived reactive oxygen species (ROS) positively regulate myotube formation (Youm et al., 2019), which may be important for muscle regeneration.

Pathway analysis of decreased genes in microgravity highlights significant changes in biological processes, including genes involved in cell adhesion and cell fate decision pathways, including Wnt and Notch signaling pathway (Figure 3F). The top 20 downregulated genes included those involved in cell adhesion (protocadherin gamma C3 [*PCDHGC3*], transforming growth factor β

Please cite this article in press as: Kim et al., Skeletal muscle-on-a-chip in microgravity as a platform for regeneration modeling and drug screening, Stem Cell Reports (2024), https://doi.org/10.1016/j.stemcr.2024.06.010

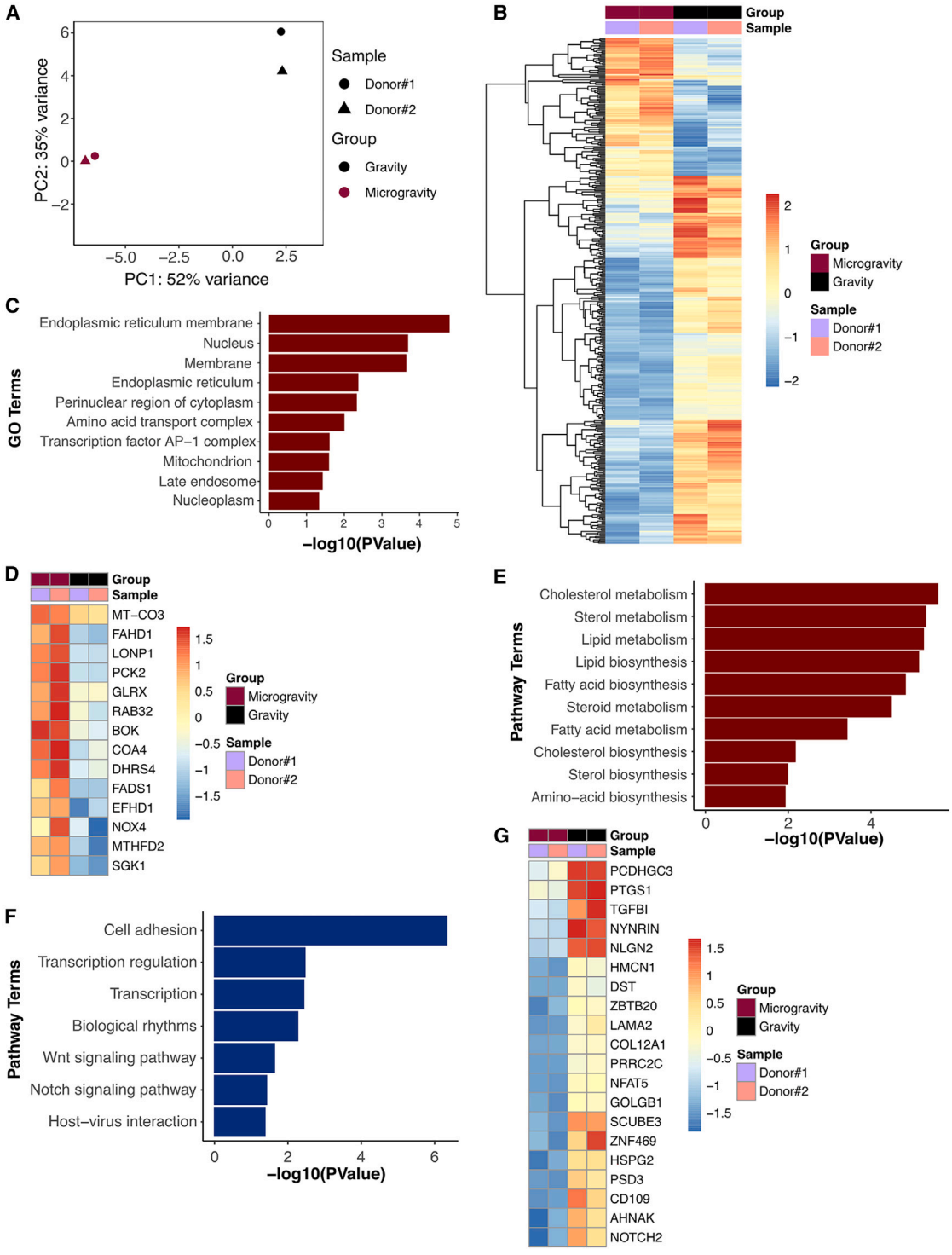

Figure 3. Transcriptional differences between microgravity and gravity control biomimetic skeletal muscle

(A) Principal-component analysis of the transcriptome of biomimetic skeletal muscle samples after 7 days in microgravity or control conditions (gravity).

(B) Heatmap shows all differentially expressed genes after 7 days in microgravity, compared to gravity (FDR 10%).

(C) Gene Ontology (GO) enrichment terms of differentially upregulated genes in microgravity ($p < 0.05$).

(legend continued on next page)

induced [*TGFBI*], neuroligin 2 [*NLGN2*], dystonin [*DST*], laminin α2 [*LAMA2*], collagen type XII alpha 1 chain [*COL12A1*]), Notch signaling pathway (*NOTCH2*), and inflammation (prostaglandin-endoperoxide synthase 1 [*PTGS1*/*COX1*]) (Figure 3G). In particular, *NOTCH2*, which is an important marker of muscle stem cell self-renewal and stem cell fate decision (Yartseva et al., 2020), was significantly downregulated in microgravity. Downregulation of *NOTCH2* gene expression in satellite cells leads to a decrease in their ability to differentiate (Fujimaki et al., 2018), suggesting an impairment in the balance between proliferation and differentiation of primary human skeletal muscle cells in microgravity. The downregulation of *NOTCH2* concurs with our *in vitro* findings of a significantly lower fusion index in the engineered muscles in microgravity (Figure S2). Additionally, extracellular matrix (ECM) remodeling is associated with muscle regeneration (Calve et al., 2010), and we observed significant downregulation of ECMs such as *COL12A1*, *LAMA2*, and heparan sulfate proteoglycan 2 (*HSPG2*) genes. Together, this analysis suggested that microgravity conditions induced a cellular phenotype that is associated with hallmarks of impaired regeneration, including metabolic remodeling, imbalance between proliferation and differentiation, and decreased cell-cell and cell-ECM adhesion.

To further examine the effects of microgravity, we performed proteomic analysis of 200 proteins from the conditioned media of bioconstructs cultured in microgravity or gravity conditions for 7 days. In comparing the microgravity versus gravity samples with FDR <25%, we identified 5 proteins that were secreted in greater abundance and 4 proteins that were of reduced abundance. The proteins of greater abundance in microgravity include Eotaxin-3 (CCL26), C-X-C motif chemokine ligand 16 (CXCL16), growth differentiation factor 15 (GDF-15), tumor necrosis factor superfamily member 14 (LIGHT/TNSF14), and pupoid fetus (PF). Of these proteins, CCL26 and CXCL16 are chemoattractants known to induce immune cell infiltration and are associated with chronic inflammation (Scholz et al., 2007; Yamada et al., 2019). In addition, GDF-15 is a biomarker for mitochondrial dysfunction and cellular senescence (Fujita et al., 2016). The proteins of reduced abundance in microgravity include bone morphogenetic protein 4 (BMP-4), Resistin, C-X-C motif chemokine ligand 12 (CXCL12/SDF-1b), interleukin-16 (IL-16), and CD40. CXCL12, in particular, is an important player in the maintenance of muscle and myogenesis (Gilbert et al., 2019; Puchert et al., 2016).

To determine whether the secreted proteomes were related to their RNA expression levels, we compared their relative expression between microgravity and gravity samples. We observed that some differential protein changes generally correlated with their corresponding RNA expression level changes (Figure S3). For example, GDF-15 was consistently increased in microgravity conditions at both the protein and RNA levels (Figure S3), whereas BMP-4 and SDF-1b (CXCL12) levels were consistently downregulated in microgravity at both the protein and RNA levels (Figure S3). Since GDF-15 has previously been reported as a diagnostic biomarker for conditions associated with impaired muscle regeneration such as aging (Ito et al., 2018; Kim et al., 2020), we searched for potential interacting genes of GDF-15 in microgravity samples. The protein-protein interaction (PPI) network was constructed by the STRING database using 107 genes that were upregulated with microgravity, including GDF-15. The unconnected genes were then removed. The resulting PPI network contained 57 nodes and 135 edges (Figure S4), where a node represents a gene and an edge represents the relationship between the two inter-connected genes. From this analysis, we identified early growth response factor 1 (EGR1) and tribbles homolog 3 (TRIB3) as the first neighbors of GDF-15. These results suggest that GDF-15 and its immediate neighbors may play an important role in microgravity-induced impairment in myogenesis.

Microgravity partially mimics genomic features of impaired muscle regeneration in sarcopenia

Since impaired muscle regeneration is associated with clinical conditions such as sarcopenia, we assessed whether the muscle-on-a-chip in microgravity platform mimics regeneration-related signaling pathways in clinical sarcopenia muscle samples. We compared the transcriptome of human muscle tissue obtained from either healthy donors (denoted as "Normal"; [n = 4]), or those with sarcopenia, as defined by accepted cutoffs for the relative skeletal muscle (RSM) index (n = 4, Table S3; Figure 4A). RNA-seq detected 58,735 genes, of which 29,313 passed the threshold for expression. In particular, 48 genes were upregulated and 113 genes were downregulated in sarcopenia samples with an FDR <25% (Figure 4B; Table S4). Among the top upregulated genes were those involved in apoptotic signaling pathways in response to DNA damage (Apoptosis enhancing nuclease [*AEN*] and *PHLDA3*), ECM organization (*TIMP1*, *COL1A1*, and *COL14A1*), and the VEGFA/VEGFR2 signaling pathway (*GIPC1*, *CTGF*, *GPC1*, and

(D) Heatmap shows the expression of genes found in the mitochondrion GO enrichment term.
(E) Pathway enrichment terms of differentially upregulated genes in microgravity (p < 0.05).
(F) Pathway enrichment terms of differentially downregulated genes in microgravity (p < 0.05).
(G) Heatmap shows expression of top 20 differentially downregulated genes in microgravity (n = 2 donors per group).

Please cite this article in press as: Kim et al., Skeletal muscle-on-a-chip in microgravity as a platform for regeneration modeling and drug screening, Stem Cell Reports (2024), https://doi.org/10.1016/j.stemcr.2024.06.010

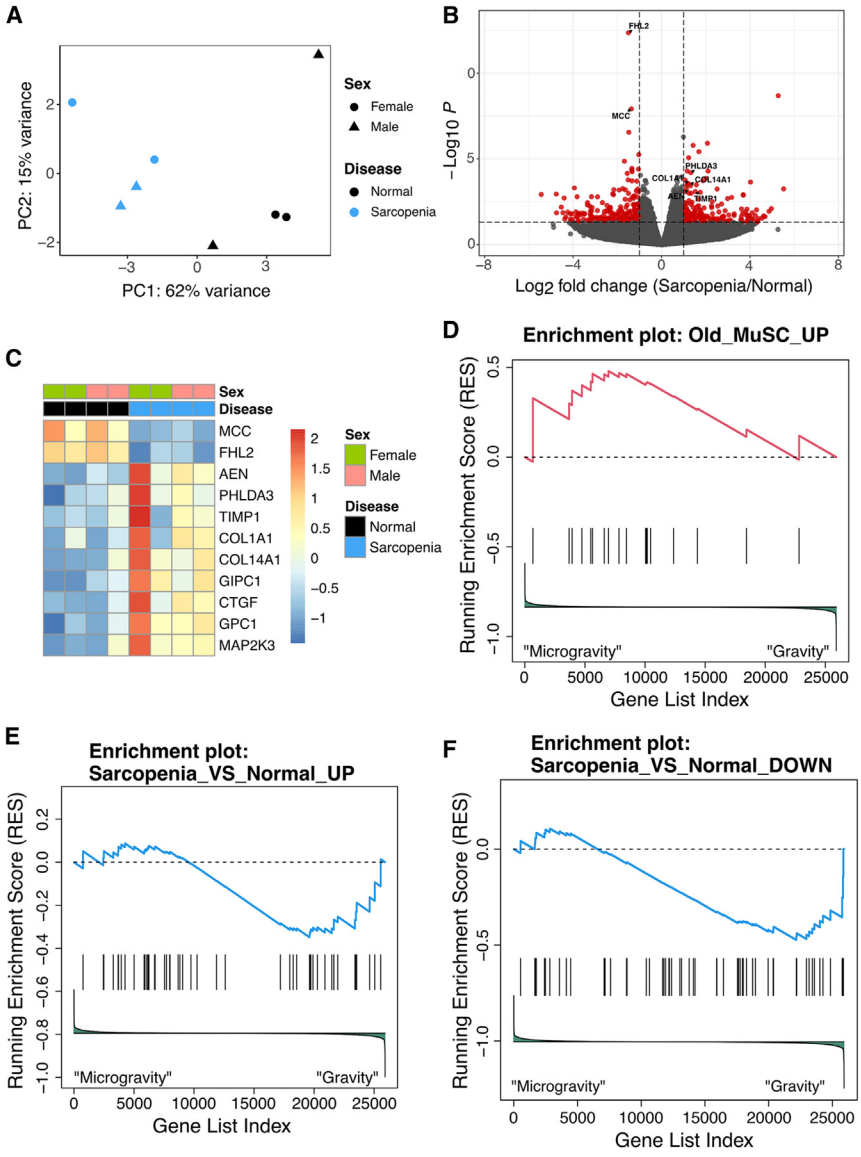

Figure 4. Transcriptional similarities between clinical sarcopenia muscle and engineered skeletal muscle in microgravity

(A) Principal-component analysis of the transcriptome in healthy vs. sarcopenia clinical samples from both sexes.

(B) Volcano plot shows differentially expressed genes in sarcopenia, compared to normal conditions ($p < 0.05$, log2 FC > 1.0). Genes involved in DNA damage response, extracellular matrix organization, VEGFA-VEGFR2 signaling pathway, and Wnt signaling are labeled. Genes showing statistically significant expression (FDR 25%) are indicated in red.

(C) Heatmap shows the genes involved in Wnt signaling, rhabdomyosarcoma, DNA damage response, extracellular matrix organization, and VEGFA-VEGFR2 signaling.

(D–F) Enrichment plots for custom gene set enrichment analysis (GSEA). The plots report positive enrichment of Old_MuSC_UP gene set (D) and negative enrichment of Sarcopenia_UP and Sarcopenia-DOWN gene sets (E–F) in microgravity, compared to gravity samples. The enrichment plot shows the gene set names (top) and the running enrichment score. The red curve indicates positive enrichment, whereas the blue curve indicates negative enrichment scores. Black bars indicate the positions of the gene set on the rank-ordered list in GSEA, and the signal-to-noise metrics are shown at the bottom.

MAP2K3). Interestingly, more genes were downregulated in sarcopenia and they included genes that are implicated in Wnt signaling (mutated in colorectal cancers [*MCC*]) and associated with rhabdomyosarcoma (*FHL2*) (Figure 4C). Importantly, an increase in apoptosis or impairment in skeletal muscle cell function could contribute to the development or progression of sarcopenia (Chung and Ng, 2006; Leeuwenburgh, 2003; Siu et al., 2005), in which the upregulation of markers such as *AEN* and *PHLDA3* is implicated in p53-dependent apoptosis (Cruz-Jentoft and Sayer, 2019; Kawase et al., 2008, 2009).

We next established a custom gene set library to assess whether engineered muscle in microgravity mimics features of sarcopenia from clinical samples. In brief, we used the up- and downregulated gene list from sarcopenia versus normal samples and converted the list into a gene set enrichment analysis (GSEA) analysis-compatible format. We also analyzed publicly available datasets derived from old adult muscle myoblasts (Gene Expression Omnibus repository: GSE52699) and generated an enriched gene set list compared to young myoblasts (see Supplemental Information). As shown in Figure 4D, custom GSEA results indicate that genes upregulated in old human myoblasts ("Old_MuSC_UP" gene set) were over-represented in the muscle-on-a-chip bioconstruct in microgravity, as indicated by the positive running enrichment score (RES) (Figure 4D). Although some of the sarcopenia-related genes were significantly decreased

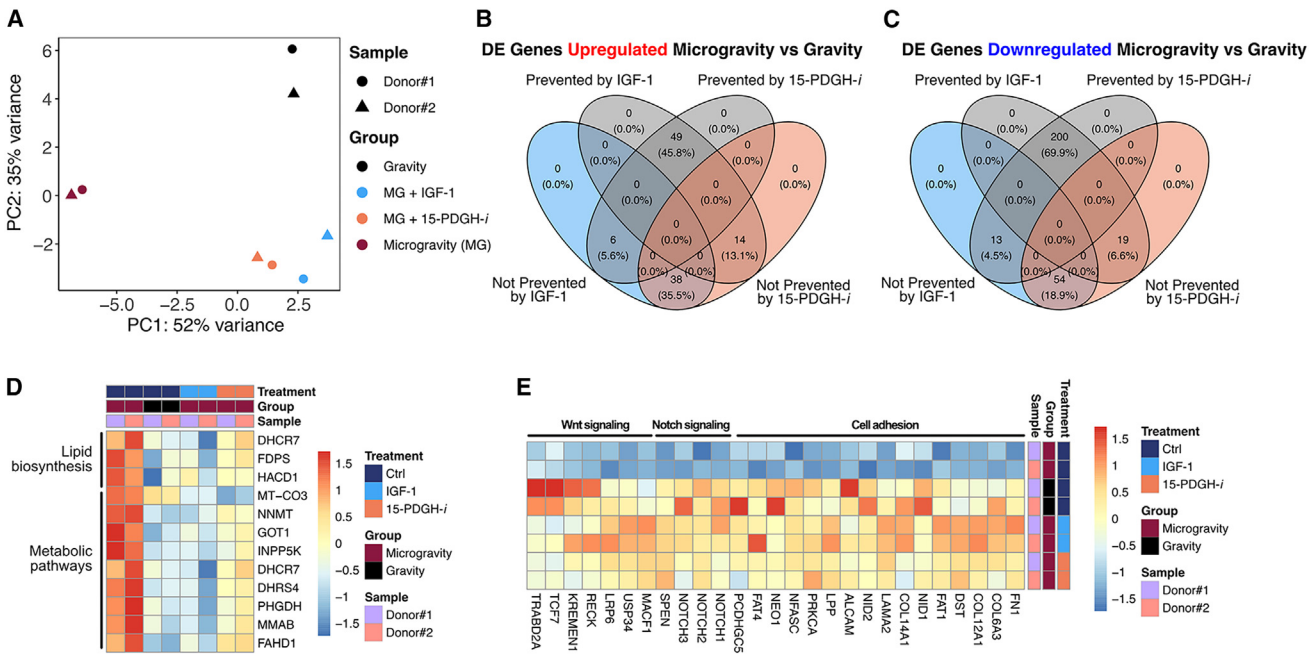

Figure 5. IGF-1 and 15-PDGFH inhibitor treatment can partially prevent microgravity effect

(A) Principal-component analysis of transcriptome in 7 days in microgravity (MG) or gravity control conditions in the presence of drug treatment (IGF-1 or 15-PDGH-*i*) in biomimetic skeletal muscle samples.

(B) The 4-way Venn diagram shows the number of differentially expressed genes that were upregulated in microgravity, compared to gravity conditions, or whose differential expression could be either prevented by IGF-1 or 15-PDGH-*i* treatment (gray) or not prevented by drug treatment (IGF-1 in blue and 15-PDGH-*i* in orange).

(C) 4-way Venn diagram showing the number of differentially expressed genes downregulated in microgravity, compared to gravity conditions, or whose differential expression could be either prevented by IGF-1 or 15-PDGH-*i* treatment (gray) or not prevented by drug treatment (IGF-1 in blue and 15-PDGH-*i* in orange).

(D) Heatmap showing genes implicated in lipid biosynthesis, metabolic pathways, and adipogenesis.

(E) Heatmap showing genes implicated in cell adhesion, Notch signaling, and Wnt signaling (n = 2 donors per group).

in gravity, compared to microgravity conditions, the enrichment plot for Sarcopenia_vs_Normal_UP shown in Figure 4E suggests that the genes upregulated by sarcopenia were not enriched by microgravity. However, the genes downregulated by sarcopenia were also downregulated with microgravity exposure (Figure 4F). These custom GSEA results indicate that the muscle-on-a-chip bioconstructs in microgravity had a negative enrichment of genes that were downregulated in sarcopenia ("Sarcopenia_VS_Normal_DOWN" gene set [Figures 4E and 4F]). These data reveal a similarity in the transcriptional signature between the clinical sarcopenia samples and engineered muscle in microgravity samples, in which the genes that were downregulated in sarcopenia muscle tissue were also downregulated in the engineered muscle in microgravity conditions, compared to those of the gravity condition (Figure 4F). Conversely, the genes that were upregulated in sarcopenia were not enriched in the microgravity condition compared to those of gravity conditions (Figure 4E). Overall, the custom GSEA results suggest that space flight mimics in part the genomic signature of old adult myoblasts and sarcopenia.

Drug treatment partially prevents adverse effects of microgravity

We next used the muscle-on-a-chip platform to perform proof-of-concept drug screening studies. Recently published studies showed that a 15-PDGH inhibitor (15-PDGH-*i*) could stimulate myogenesis as well as abrogate sarcopenia in preclinical models through the regulation of prostaglandin E_2 signaling (Ho et al., 2017; Palla et al., 2021). Besides 15-PDGH-*i*, we also examined insulin-like growth factor-1 (IGF-1) in the muscle-on-a-chip platform. The effects of IGF-1 in promoting muscle myogenesis and inhibition of muscle atrophy are well established (Alcazar et al., 2020; Ascenzi et al., 2019; Ma et al., 2009; Machida and Booth, 2004; Yu et al., 2015). To examine the potential use of these two drugs to regulate myogenesis, the engineered skeletal muscle-on-a-chip bioconstructs were treated with either IGF-1 or 15-PDGH-*i* for 7 days in

Please cite this article in press as: Kim et al., Skeletal muscle-on-a-chip in microgravity as a platform for regeneration modeling and drug screening, Stem Cell Reports (2024), https://doi.org/10.1016/j.stemcr.2024.06.010

microgravity conditions, followed by RNA-seq analysis. Through principal-component analysis, we found that, in microgravity, the drug-treated groups were generally more transcriptionally similar to the samples in gravity, rather than their microgravity counterparts (Figure 5A). Out of 107 genes that were upregulated in microgravity compared to gravity counterparts, 49 genes showed similar expression levels to those of gravity conditions with IGF-1 and 15-PDGH-*i* treatment, suggesting that the drugs could prevent the transcriptional upregulation effects of microgravity. In addition, IGF-1 and 15-PDGH-*i* treatment prevented the transcriptional upregulation effects of microgravity in 6 and 14 genes, respectively (Figure 5B).

Of the 286 downregulated genes with microgravity, 200 genes showed similar expression levels to those of gravity conditions with IGF-1 and 15-PDGH-*i* treatment, suggesting that the drugs could prevent the transcriptional downregulation effects of microgravity. In particular, IGF-1 and 15-PDGH-*i* treatment prevented the transcriptional downregulation effects of microgravity of 13 genes and 19 genes, respectively (Figure 5C). As noted earlier, pathway enrichment analysis highlighted an enrichment of genes associated with metabolic pathways including lipid and fatty acid metabolism in microgravity samples. We found that the drug treatment prevented a shift in metabolic profiles and maintained normal expression of genes involved in lipid biosynthesis (*DHCR7*, *FDPS*, *HACD1*) and metabolic pathways (*MT-CO3*, *NNMT*, *GOT1*, *INPP5K*, *DHCR7*, *DHRS4*, *PHGDH*, *MMAB*, *FAHD1*) (Figure 5D). Moreover, we also observed that many genes implicated in cell adhesion, the Notch signaling pathway (*NOTCH1*, *NOTCH2*, *NOTCH3*, *SPEN*), and the Wnt signaling pathway (*MACF1*, *USP34*, *LRP6*, *RECK*, *KREMEN1*, *TCF7*, *TRABD2A*) were downregulated with space flight but were similar in expression level to gravity samples upon drug treatment (Figures 5E, S5A, and S5B). Overall, the drug-treated samples displayed a signature that more closely resembled gravity samples, compared to their microgravity counterparts.

Since the addition of IGF-1 and 15-PDGH-*i* prevented some effects of microgravity at the transcriptional level, we further assessed their effect on proteins found in conditioned media at 7 days after drug treatment. Interestingly, we found that IGF-1 and 15-PDGH-*i* treatment prevented the ability of microgravity to increase GDF-15 protein levels (Figure S5C; Table S5). Additionally, 15-PDGH-*i* treatment protected CXCL16 and PF4 protein levels from rising to levels, similar to those of microgravity samples. Despite the ability of the drugs to prevent an increase in protein levels to reach those of microgravity samples, none of the proteins that were decreased in microgravity compared to gravity conditions could be normalized to the levels associated with gravity samples by the addition of drugs (Figure S5D). We further tested whether the first neighbors of GDF-15 (EGR1 and TRIB3) are affected with drug treatment. As described earlier, EGR1 was not affected by drug treatment, whereas IGF-1 addition prevented TRIB3 level from reaching that of microgravity samples (Figure S5E). Taken together, our multi-omics analysis demonstrates that microgravity induces in engineered muscle a signature that reflects salient aspects of impaired myogenesis, which could be partially prevented by IGF-1 or 15-PDGH-*i*.

DISCUSSION

The salient findings of the work are the following: (1) an engineered muscle-on-a-chip platform facilitates the study of microgravity effects on myotube formation and muscle-related biological processes; (2) microgravity mimics salient aspects of impaired regeneration, based on RNA-seq and proteomic analysis; (3) microgravity effects on engineered muscle can be prevented in part by IGF-1 and PDGH-*i* addition; and (4) drug screening in microgravity using an engineered muscle-on-a-chip platform is feasible. These findings suggest that aspects of impaired muscle myogenesis can be modeled in just one week of exposure in microgravity and that drug screening in microgravity may be a useful platform for identifying potential drug targets that regulate myogenesis.

The study of the effects of microgravity on engineered muscle-on-a-chip is an emerging area of research. Our findings using engineered muscle in microgravity concur with Vandenburgh et al., whose engineered avian muscle aboard the Space Transportation Shuttle for 12 days showed evidence of reduced myofiber size and cross-sectional area (Vandenburgh et al., 1999). Additionally, a larger body of work derived from *in vitro* cultured myoblasts in microgravity or simulated microgravity further supports the finding that microgravity abrogates myogenic differentiation and myotube size, owing to cellular senescence and epigenetic modifications (Furukawa et al., 2018; Parafati et al., 2023; Takahashi et al., 2021). Our findings of impaired myotube formation in the presence of microgravity are in alignment with these studies.

Previous studies have reported multiple effects of spaceflight on human physiology. Most recently, large-scale multi-omics, systems biology analytical approaches profiled 59 astronauts from the National Aeronautics and Space Administration (NASA)'s GeneLab to determine transcriptomic, proteomic, metabolomic, and epigenetic responses to spaceflight, which highlighted a significant enrichment for mitochondrial processes and DNA damage (da Silveira et al., 2020). Alterations in mitochondrial activity and impaired lipid metabolism are associated with muscle atrophy (Nikawa et al., 2004; Vitry et al., 2022). In line with

Please cite this article in press as: Kim et al., Skeletal muscle-on-a-chip in microgravity as a platform for regeneration modeling and drug screening, Stem Cell Reports (2024), https://doi.org/10.1016/j.stemcr.2024.06.010

these reports, our engineered muscle-on-a-chip platform exposed to microgravity for 7 days also demonstrated changes in mitochondrial genes (Figure 3C), a shift in metabolism toward lipid and fatty acid biosynthesis (Figure 3E), and an increase in apoptotic processes (*BOK*, *SGK1*, and *NOX4*). The existence of mitochondrial dysfunction was further supported by proteomic studies reporting an increase in GDF-15. GDF-15 is a biomarker of dysfunctional mitochondria and cellular senescence (Fujita et al., 2016). Increased GDF-15 levels are associated with muscle atrophy in cancer models, and GDF-15 treatment was shown to induce muscle atrophy in C2C12 myotubes (Zhang et al., 2022). GDF-15 neutralization could restore muscle mass and function (Kim-Muller et al., 2023). More importantly, the addition of pro-regenerative drugs such as IGF-1 and 15-PGDH-*i* could partially prevent the effects of microgravity on our engineered muscle-on-a-chip platform.

Notch signaling is major regulator of myogenesis (Luo et al., 2005). The disruption in Notch signaling in aging muscle compromises new myofiber formation and impairs tissue regeneration as a potential contributing factor to sarcopenia (Arthur and Cooley, 2012; Carlson et al., 2008; Conboy et al., 2003). Notch inhibition also contributes to the dysregulation of cellular quiescence and can perturb the quiescent state of the muscle stem cells (Bjornson et al., 2012; van Velthoven and Rando, 2019). Notch signaling can also regulate the stability of a tumor suppressor, p53. The Notch-p53 axis declines with age and is detrimental to cell survival and expansion (Liu et al., 2018). Our data are consistent with the literature in demonstrating a downregulation in Notch signaling in microgravity (Figure 3F). The loss of such a signal is correlated with reduced differentiation potential, as demonstrated by the impairment in myotube formation.

More genes were downregulated than upregulated in both microgravity versus gravityand the comparison of sarcopenia versus normal muscle samples. Microgravity samples were more sarcopenia like in terms of genes that are important for apoptosis and Wnt signaling. The genes involved in apoptosis were upregulated, whereas the genes involved in Wnt signaling were downregulated in both microgravity and sarcopenia samples. Although the cellular response to gamma radiation and apoptosis processes increased with microgravity but were not prevented with IGF-1 or 15-PGDH-*i* treatment, the gene expression of Wnt signaling components including *Lrp6* was prevented with drug treatment (Figure 5E). *Lrp6* is one of the two co-receptors involved in canonical Wnt signaling in vertebrates and conditional *Lrp6* knockout reduced fiber size in mice (Gessler et al., 2022; Ren et al., 2021), highlighting its importance in muscle mass maintenance. Interestingly, microgravity increased the expression level of TRIB3, which negatively regulates cell survival and inhibits myogenic differentiation (Kato and Du, 2007; Saleem and Biswas, 2017). TRIB3 was identified in the PPI network as one of the two immediate neighboring gene of GDF-15. IGF-1 treatment prevented the elevation of TRIB3 gene expression in microgravity. In a mouse model, *Trib3* is implicated in both age-related and food deprivation-induced muscle fiber atrophy and fibrosis (Choi et al., 2019; Shang et al., 2020). Furthermore, our findings align with a recent report that also demonstrated differential expression of *TRIB3* and *PCK2* under microgravity conditions (Parafati et al., 2023), further supporting the impact of microgravity on myogenesis and metabolism.

We acknowledge the limitations associated with this study. Owing to constraints associated with space research, only one launch was possible. For this reason, the data were derived from two primary human muscle donors as a measure of variance in the dataset. Furthermore, we acknowledge that measurements of muscle contractility could be informative, but such a functional assay would be most appropriate for engineered muscles that are more mature, which would have further increased the duration of the studies. Finally, the findings from the data in microgravity do not preclude the possibility of other contributing factors such as ionizing radiation. Despite these limitations, we believe that the observed effects of microgravity on engineered muscle are compelling and provide an avenue for future drug screening explorations in space for identifying drug targets that can enhance muscle myogenesis.

In conclusion, we show that engineered muscle-on-a-chip bioconstructs exposed to microgravity induced prominent changes to their transcriptome that mimic aspects of impaired myogenesis. GSEA demonstrated a shift in metabolic pathways toward lipid metabolism, along with downregulated Notch signaling pathways and the increased expression of apoptotic genes. Importantly, microgravity exposure to engineered muscle-on-a-chip bioconstructs resembled some similar features to that of clinical sarcopenia muscle. The effects of microgravity could be partly prevented by the addition of IGF-1 or a 15-PGDH-*i*. Together, this transcriptomic and proteomics analyses of microgravity effects using a muscle-on-a-chip platform demonstrate that microgravity mimics aspects of impaired myogenesis. This work further highlights the utility of microgravity as a unique environment for drug discovery.

EXPERIMENTAL PROCEDURES

Resource availability

Lead contact

Further information and requests for resources and reagents should be directed to and will be fulfilled by the lead contact, Ngan F. Huang (ngantina@stanford.edu).

Materials availability

This study did not generate new unique reagents.

Data and code availability

The accession number for the RNA-seq raw data reported in this paper is GSE238215. The accession number will be accesible to readers upon publication. All data may be made available by request to the corresponding author.

Flight experiment in microgravity

The experiments were initiated in microgravity with the exchange of media into induction media consisting of DMEM supplemented with 2% horse serum and 1% penicillin/streptomycin (day 0), according to Figure 2B. The media were exchanged again on day 3. The viability of samples was qualitatively monitored using an on-orbit phase-contrast microscope (Figure S1F). On day 7, the conditioned media within the bioreactors were harvested and stored at −80°C. The muscle-on-a-chip devices within each chamber were either treated with RNAlater stabilization agent (Fisher Scientific) and then stored at −80°C or fixed in 4% paraformaldehyde (Fisher Scientific) for 15 min and then stored at 4°C. Samples were maintained on the ISSNL at the indicated temperatures and then returned to Earth on SpaceX Cargo Resupply Service 23 about two months later. Semi-synchronous ground control experiments were performed on a separate set of muscle-on-a-chip bioconstructs from the same donors in identical bioreactors and syringe media exchange procedures. The bioreactors in normal gravity conditions were cultured in conventional incubators but were handled otherwise in the same manner and with the same time stamps, as in microgravity.

Statistical analysis

Statistical analysis of transcriptional and proteomics data is described earlier or in the supplemental experimental procedures. Where applicable, data are shown as mean ± standard deviation. Statistical significance was accepted at $p < 0.05$.

SUPPLEMENTAL INFORMATION

Supplemental information can be found online at https://doi.org/10.1016/j.stemcr.2024.06.010.

ACKNOWLEDGMENTS

This work was supported in part by grants to N.F.H. from the US National Institutes of Health (R01 HL142718, R41 HL170875, and R21 HL172096-01), the US Department of Veterans Affairs (1I01BX004259, 5I01RX001222, and 1I21RX004898), the National Science Foundation (1829534 and 2227614), the Center for the Advancement of Science in Space (CASIS, 80JSC018M0005), and the American Heart Association (20IPA35360085 and 20IPA35310731) and by grants to T.A.R. from the US National Institutes of Health (R01 AG068667 and P01 AG036695) and the US Department of Veterans Affairs (I01BX002324 and I01RX001222). N.F.H. is a recipient of a Research Career Scientist award (IK6 BX006309) from the Department of Veterans Affairs. We acknowledge the technical assistance of astronauts, namely, Thomas Pesquet, K. Megan McArthur, and Mark Vande Hei who performed the experiments on the ISSNL. We also acknowledge members from BioServe Space Technologies for technical and logistical support associated with the launch, namely Matthew Vellone, Shankini Doraisingam, Mark Rupert, Stefanie Countryman, and Sheila Murphy. We acknowledge project management assistance of Kristin Kopperud and Marc Giulianotti from CASIS. Finally, we acknowledge the clinical muscle RNA samples from the University of Kentucky Center for Muscle Biology. Figures 1 and 2, and the graphical abstract were created with Biorender.com.

AUTHOR CONTRIBUTIONS

Conceptualization: N.F.H. and T.A.R. Funding acquisition: N.F.H. and T.A.R. Methodology: B.A., M.S., T.A.R., and N.F.H. Investigation: S.K., B.A., and M.S. Resources: N.F.H. and T.A.R. Supervision: N.F.H. and T.A.R. Visualization: S.K., B.A., and M.S. Writing – original draft: S.K. and N.F.H. Writing – review and editing: S.K., B.A., M.S., T.A.R., and N.F.H.

DECLARATION OF INTERESTS

The authors declare no competing interests.

Received: December 29, 2023
Revised: June 22, 2024
Accepted: June 23, 2024
Published: July 25, 2024

REFERENCES

Alcazar, C.A., Hu, C., Rando, T.A., Huang, N.F., and Nakayama, K.H. (2020). Transplantation of insulin-like growth factor-1 laden scaffolds combined with exercise promotes neuroregeneration and angiogenesis in a preclinical muscle injury model. Biomater. Sci. *8*, 5376–5389. https://doi.org/10.1039/d0bm00990c.

Andres-Mateos, E., Brinkmeier, H., Burks, T.N., Mejias, R., Files, D.C., Steinberger, M., Soleimani, A., Marx, R., Simmers, J.L., Lin, B., et al. (2013). Activation of serum/glucocorticoid-induced kinase 1 (SGK1) is important to maintain skeletal muscle homeostasis and prevent atrophy. EMBO Mol. Med. *5*, 80–91. https://doi.org/10.1002/emmm.201201443.

Arthur, S.T., and Cooley, I.D. (2012). The effect of physiological stimuli on sarcopenia; impact of Notch and Wnt signaling on impaired aged skeletal muscle repair. Int. J. Biol. Sci. *8*, 731–760. https://doi.org/10.7150/ijbs.4262.

Ascenzi, F., Barberi, L., Dobrowolny, G., Villa Nova Bacurau, A., Nicoletti, C., Rizzuto, E., Rosenthal, N., Scicchitano, B.M., and Musaro, A. (2019). Effects of IGF-1 isoforms on muscle growth and sarcopenia. Aging Cell *18*, e12954. https://doi.org/10.1111/acel.12954.

Bjornson, C.R., Cheung, T.H., Liu, L., Tripathi, P.V., Steeper, K.M., and Rando, T.A. (2012). Notch signaling is necessary to maintain quiescence in adult muscle stem cells. Stem Cell. *30*, 232–242. https://doi.org/10.1002/stem.773.

Calve, S., Odelberg, S.J., and Simon, H.G. (2010). A transitional extracellular matrix instructs cell behavior during muscle regeneration. Dev. Biol. *344*, 259–271. https://doi.org/10.1016/j.ydbio.2010.05.007.

Carlson, M.E., Hsu, M., and Conboy, I.M. (2008). Imbalance between pSmad3 and Notch induces CDK inhibitors in old muscle stem cells. Nature *454*, 528–532. https://doi.org/10.1038/nature07034.

Choi, R.H., McConahay, A., Silvestre, J.G., Moriscot, A.S., Carson, J.A., and Koh, H.J. (2019). TRB3 regulates skeletal muscle mass in food deprivation-induced atrophy. FASEB J. *33*, 5654–5666. https://doi.org/10.1096/fj.201802145RR.

Chung, L., and Ng, Y.C. (2006). Age-related alterations in expression of apoptosis regulatory proteins and heat shock proteins in rat skeletal muscle. Biochim. Biophys. Acta *1762*, 103–109. https://doi.org/10.1016/j.bbadis.2005.08.003.

Conboy, I.M., Conboy, M.J., Smythe, G.M., and Rando, T.A. (2003). Notch-mediated restoration of regenerative potential to aged muscle. Science *302*, 1575–1577. https://doi.org/10.1126/science.1087573.

Cruz-Jentoft, A.J., and Sayer, A.A. (2019). Sarcopenia. Lancet *393*, 2636–2646. https://doi.org/10.1016/S0140-6736(19)31138-9.

da Silveira, W.A., Fazelinia, H., Rosenthal, S.B., Laiakis, E.C., Kim, M.S., Meydan, C., Kidane, Y., Rathi, K.S., Smith, S.M., Stear, B., et al. (2020). Comprehensive Multi-omics Analysis Reveals Mitochondrial Stress as a Central Biological Hub for Spaceflight Impact. Cell *183*, 1185–1201.e20. https://doi.org/10.1016/j.cell.2020.11.002.

Dehner, M., Hadjihannas, M., Weiske, J., Huber, O., and Behrens, J. (2008). Wnt signaling inhibits Forkhead box O3a-induced transcription and apoptosis through up-regulation of serum- and glucocorticoid-inducible kinase 1. J. Biol. Chem. *283*, 19201–19210. https://doi.org/10.1074/jbc.M710366200.

Fitts, R.H., Trappe, S.W., Costill, D.L., Gallagher, P.M., Creer, A.C., Colloton, P.A., Peters, J.R., Romatowski, J.G., Bain, J.L., and Riley, D.A. (2010). Prolonged space flight-induced alterations in the structure and function of human skeletal muscle fibres. J. Physiol. *588*, 3567–3592. https://doi.org/10.1113/jphysiol.2010.188508.

Fujimaki, S., Seko, D., Kitajima, Y., Yoshioka, K., Tsuchiya, Y., Masuda, S., and Ono, Y. (2018). Notch1 and Notch2 Coordinately Regulate Stem Cell Function in the Quiescent and Activated States of Muscle Satellite Cells. Stem Cell. *36*, 278–285. https://doi.org/10.1002/stem.2743.

Fujita, Y., Taniguchi, Y., Shinkai, S., Tanaka, M., and Ito, M. (2016). Secreted growth differentiation factor 15 as a potential biomarker for mitochondrial dysfunctions in aging and age-related disorders. Geriatr. Gerontol. Int. *16*, 17–29. https://doi.org/10.1111/ggi.12724.

Furukawa, T., Tanimoto, K., Fukazawa, T., Imura, T., Kawahara, Y., and Yuge, L. (2018). Simulated microgravity attenuates myogenic differentiation via epigenetic regulations. NPJ Microgravity *4*, 11. https://doi.org/10.1038/s41526-018-0045-0.

Gessler, L., Kurtek, C., Merholz, M., Jian, Y., and Hashemolhosseini, S. (2022). In Adult Skeletal Muscles, the Co-Receptors of Canonical Wnt Signaling, Lrp5 and Lrp6, Determine the Distribution and Size of Fiber Types, and Structure and Function of Neuromuscular Junctions. Cells *11*, 3698. https://doi.org/10.3390/cells11243968.

Gilbert, W., Bragg, R., Elmansi, A.M., McGee-Lawrence, M.E., Isales, C.M., Hamrick, M.W., Hill, W.D., and Fulzele, S. (2019). Stromal cell-derived factor-1 (CXCL12) and its role in bone and muscle biology. Cytokine *123*, 154783. https://doi.org/10.1016/j.cyto.2019.154783.

Ho, A.T.V., Palla, A.R., Blake, M.R., Yucel, N.D., Wang, Y.X., Magnusson, K.E.G., Holbrook, C.A., Kraft, P.E., Delp, S.L., and Blau, H.M. (2017). Prostaglandin E2 is essential for efficacious skeletal muscle stem-cell function, augmenting regeneration and strength. Proc. Natl. Acad. Sci. USA *114*, 6675–6684. https://doi.org/10.1073/pnas.1705420114.

Huang, N.F., Patel, S., Thakar, R.G., Wu, J., Hsiao, B.S., Chu, B., Lee, R.J., and Li, S. (2006). Myotube assembly on nanofibrous and micropatterned polymers. Nano Lett. *6*, 537–542. https://doi.org/10.1021/nl060060o.

Huang, S., Wang, X., Yu, J., Tian, Y., Yang, C., Chen, Y., Chen, H., and Ge, H. (2020). LonP1 regulates mitochondrial network remodeling through the PINK1/Parkin pathway during myoblast differentiation. Am J. Physiol. Cell Physiol. *319*, C1020–C1028. https://doi.org/10.1152/ajpcell.00589.2019.

Ito, T., Nakanishi, Y., Yamaji, N., Murakami, S., and Schaffer, S.W. (2018). Induction of Growth Differentiation Factor 15 in Skeletal Muscle of Old Taurine Transporter Knockout Mouse. Biol. Pharm. Bull. *41*, 435–439. https://doi.org/10.1248/bpb.b17-00969.

Juhl, O.J.t., Buettmann, E.G., Friedman, M.A., DeNapoli, R.C., Hoppock, G.A., and Donahue, H.J. (2021). Update on the effects of microgravity on the musculoskeletal system. NPJ Microgravity *7*, 28. https://doi.org/10.1038/s41526-021-00158-4.

Kato, S., and Du, K. (2007). TRB3 modulates C2C12 differentiation by interfering with Akt activation. Biochem. Biophys. Res. Commun. *353*, 933–938. https://doi.org/10.1016/j.bbrc.2006.12.161.

Kawase, T., Ichikawa, H., Ohta, T., Nozaki, N., Tashiro, F., Ohki, R., and Taya, Y. (2008). p53 target gene AEN is a nuclear exonuclease required for p53-dependent apoptosis. Oncogene *27*, 3797–3810. https://doi.org/10.1038/onc.2008.32.

Kawase, T., Ohki, R., Shibata, T., Tsutsumi, S., Kamimura, N., Inazawa, J., Ohta, T., Ichikawa, H., Aburatani, H., Tashiro, F., and Taya, Y. (2009). PH domain-only protein PHLDA3 is a p53-regulated repressor of Akt. Cell *136*, 535–550. https://doi.org/10.1016/j.cell.2008.12.002.

Kim-Muller, J.Y., Song, L., LaCarubba Paulhus, B., Pashos, E., Li, X., Rinaldi, A., Joaquim, S., Stansfield, J.C., Zhang, J., Robertson, A., et al. (2023). GDF15 neutralization restores muscle function and physical performance in a mouse model of cancer cachexia. Cell Rep. *42*, 111947. https://doi.org/10.1016/j.celrep.2022.111947.

Kim, H., Kim, K.M., Kang, M.J., and Lim, S. (2020). Growth differentiation factor-15 as a biomarker for sarcopenia in aging humans and mice. Exp. Gerontol. *142*, 111115. https://doi.org/10.1016/j.exger.2020.111115.

Leeuwenburgh, C. (2003). Role of apoptosis in sarcopenia. J. Gerontol. A. Biol. Sci. Med. Sci. *58*, 999–1001. https://doi.org/10.1093/gerona/58.11.m999.

Liu, L., Charville, G.W., Cheung, T.H., Yoo, B., Santos, P.J., Schroeder, M., and Rando, T.A. (2018). Impaired Notch Signaling Leads to a Decrease in p53 Activity and Mitotic Catastrophe in

Aged Muscle Stem Cells. Cell Stem Cell *23*, 544–556.e4. https://doi.org/10.1016/j.stem.2018.08.019.

Luo, D., Renault, V.M., and Rando, T.A. (2005). The regulation of Notch signaling in muscle stem cell activation and postnatal myogenesis. Semin. Cell Dev. Biol. *16*, 612–622. https://doi.org/10.1016/j.semcdb.2005.07.002.

Ma, Q.L., Yang, T.L., Yin, J.Y., Peng, Z.Y., Yu, M., Liu, Z.Q., and Chen, F.P. (2009). Role of insulin-like growth factor-1 (IGF-1) in regulating cell cycle progression. Biochem. Biophys. Res. Commun. *389*, 150–155. https://doi.org/10.1016/j.bbrc.2009.08.114.

Machida, S., and Booth, F.W. (2004). Insulin-like growth factor 1 and muscle growth: implication for satellite cell proliferation. Proc. Nutr. Soc. *63*, 337–340. https://doi.org/10.1079/PNS2004354.

Mauro, A. (1961). Satellite cell of skeletal muscle fibers. J. Biophys. Biochem. Cytol. *9*, 493–495. https://doi.org/10.1083/jcb.9.2.493.

Morgan, J.E., and Partridge, T.A. (2003). Muscle satellite cells. Int. J. Biochem. Cell Biol. *35*, 1151–1156. https://doi.org/10.1016/s1357-2725(03)00042-6.

Nakayama, K.H., Quarta, M., Paine, P., Alcazar, C., Karakikes, I., Garcia, V., Abilez, O.J., Calvo, N.S., Simmons, C.S., Rando, T.A., and Huang, N.F. (2019). Treatment of volumetric muscle loss in mice using nanofibrillar scaffolds enhances vascular organization and integration. Commun. Biol. *2*, 170. https://doi.org/10.1038/s42003-019-0416-4.

Nikawa, T., Ishidoh, K., Hirasaka, K., Ishihara, I., Ikemoto, M., Kano, M., Kominami, E., Nonaka, I., Ogawa, T., Adams, G.R., et al. (2004). Skeletal muscle gene expression in space-flown rats. FASEB J. *18*, 522–524. https://doi.org/10.1096/fj.03-0419fje.

Palla, A.R., Ravichandran, M., Wang, Y.X., Alexandrova, L., Yang, A.V., Kraft, P., Holbrook, C.A., Schurch, C.M., Ho, A.T.V., and Blau, H.M. (2021). Inhibition of prostaglandin-degrading enzyme 15-PGDH rejuvenates aged muscle mass and strength. Science *371*, abc8059. https://doi.org/10.1126/science.abc8059.

Parafati, M., Giza, S., Shenoy, T.S., Mojica-Santiago, J.A., Hopf, M., Malany, L.K., Platt, D., Moore, I., Jacobs, Z.A., Kuehl, P., et al. (2023). Human skeletal muscle tissue chip autonomous payload reveals changes in fiber type and metabolic gene expression due to spaceflight. NPJ Microgravity *9*, 77. https://doi.org/10.1038/s41526-023-00322-y.

Pedruzzi, E., Guichard, C., Ollivier, V., Driss, F., Fay, M., Prunet, C., Marie, J.C., Pouzet, C., Samadi, M., Elbim, C., et al. (2004). NAD(P)H oxidase Nox-4 mediates 7-ketocholesterol-induced endoplasmic reticulum stress and apoptosis in human aortic smooth muscle cells. Mol. Cell Biol. *24*, 10703–10717. https://doi.org/10.1128/MCB.24.24.10703-10717.2004.

Perez, K., Ciotlos, S., McGirr, J., Limbad, C., Doi, R., Nederveen, J.P., Nilsson, M.I., Winer, D.A., Evans, W., Tarnopolsky, M., et al. (2022). Single nuclei profiling identifies cell specific markers of skeletal muscle aging, frailty, and senescence. Aging (Albany NY) *14*, 9393–9422. https://doi.org/10.18632/aging.204435.

Puchert, M., Adams, V., Linke, A., and Engele, J. (2016). Evidence for the involvement of the CXCL12 system in the adaptation of skeletal muscles to physical exercise. Cell. Signal. *28*, 1205–1215. https://doi.org/10.1016/j.cellsig.2016.05.019.

Radugina, E.A., Almeida, E.A.C., Blaber, E., Poplinskaya, V.A., Markitantova, Y.V., and Grigoryan, E.N. (2018). Exposure to microgravity for 30 days onboard Bion M1 caused muscle atrophy and impaired regeneration in murine femoral Quadriceps. Life Sci. Space Res. *16*, 18–25. https://doi.org/10.1016/j.lssr.2017.08.005.

Reid, K.F., and Fielding, R.A. (2012). Skeletal muscle power: a critical determinant of physical functioning in older adults. Exerc. Sport Sci. Rev. *40*, 4–12. https://doi.org/10.1097/JES.0b013e31823b5f13.

Ren, Q., Chen, J., and Liu, Y. (2021). LRP5 and LRP6 in Wnt Signaling: Similarity and Divergence. Front. Cell Dev. Biol. *9*, 670960. https://doi.org/10.3389/fcell.2021.670960.

Ren, Z., Ahn, E.H., Do, M., Mair, D.B., Monemianesfahani, A., Lee, P.H.U., and Kim, D.H. (2024). Simulated microgravity attenuates myogenesis and contractile function of 3D engineered skeletal muscle tissues. NPJ Microgravity *10*, 18. https://doi.org/10.1038/s41526-024-00353-z.

Saleem, S., and Biswas, S.C. (2017). Tribbles Pseudokinase 3 Induces Both Apoptosis and Autophagy in Amyloid-beta-induced Neuronal Death. J. Biol. Chem. *292*, 2571–2585. https://doi.org/10.1074/jbc.M116.744730.

Scholz, F., Schulte, A., Adamski, F., Hundhausen, C., Mittag, J., Schwarz, A., Kruse, M.L., Proksch, E., and Ludwig, A. (2007). Constitutive expression and regulated release of the transmembrane chemokine CXCL16 in human and murine skin. J. Invest. Dermatol. *127*, 1444–1455. https://doi.org/10.1038/sj.jid.5700751.

Shang, G.K., Han, L., Wang, Z.H., Liu, Y.P., Yan, S.B., Sai, W.W., Wang, D., Li, Y.H., Zhang, W., and Zhong, M. (2020). Sarcopenia is attenuated by TRB3 knockout in aging mice via the alleviation of atrophy and fibrosis of skeletal muscles. J. Cachexia Sarcopenia Muscle *11*, 1104–1120. https://doi.org/10.1002/jcsm.12560.

Siu, P.M., Pistilli, E.E., and Alway, S.E. (2005). Apoptotic responses to hindlimb suspension in gastrocnemius muscles from young adult and aged rats. Am. J. Physiol. Regul. Integr. Comp. Physiol. *289*, R1015–R1026. https://doi.org/10.1152/ajpregu.00198.2005.

Takahashi, H., Nakamura, A., and Shimizu, T. (2021). Simulated microgravity accelerates aging of human skeletal muscle myoblasts at the single cell level. Biochem. Biophys. Res. Commun. *578*, 115–121. https://doi.org/10.1016/j.bbrc.2021.09.037.

Trappe, T. (2009). Influence of aging and long-term unloading on the structure and function of human skeletal muscle. Appl. Physiol. Nutr. Metab. *34*, 459–464. https://doi.org/10.1139/H09-041.

van Velthoven, C.T.J., and Rando, T.A. (2019). Stem Cell Quiescence: Dynamism, Restraint, and Cellular Idling. Cell Stem Cell *24*, 213–225. https://doi.org/10.1016/j.stem.2019.01.001.

Vandenburgh, H., Chromiak, J., Shansky, J., Del Tatto, M., and Lemaire, J. (1999). Space travel directly induces skeletal muscle atrophy. FASEB J. *13*, 1031–1038. https://doi.org/10.1096/fasebj.13.9.1031.

Vitry, G., Finch, R., McStay, G., Behesti, A., Dejean, S., Larose, T., Wotring, V., and da Silveira, W.A. (2022). Muscle atrophy phenotype gene expression during spaceflight is linked to a metabolic crosstalk in both the liver and the muscle in mice. iScience *25*, 105213. https://doi.org/10.1016/j.isci.2022.105213.

Yakovlev, A.G., Di Giovanni, S., Wang, G., Liu, W., Stoica, B., and Faden, A.I. (2004). BOK and NOXA are essential mediators of p53-dependent apoptosis. J. Biol. Chem. *279*, 28367–28374. https://doi.org/10.1074/jbc.M313526200.

Yamada, T., Miyabe, Y., Ueki, S., Fujieda, S., Tokunaga, T., Sakashita, M., Kato, Y., Ninomiya, T., Kawasaki, Y., Suzuki, S., and Saito, H. (2019). Eotaxin-3 as a Plasma Biomarker for Mucosal Eosinophil Infiltration in Chronic Rhinosinusitis. Front. Immunol. *10*, 74. https://doi.org/10.3389/fimmu.2019.00074.

Yartseva, V., Goldstein, L.D., Rodman, J., Kates, L., Chen, M.Z., Chen, Y.J., Foreman, O., Siebel, C.W., Modrusan, Z., Peterson, A.S., and Jovicic, A. (2020). Heterogeneity of Satellite Cells Implicates DELTA1/NOTCH2 Signaling in Self-Renewal. Cell Rep. *30*, 1491–1503.e6. https://doi.org/10.1016/j.celrep.2019.12.100.

Youm, T.H., Woo, S.H., Kwon, E.S., and Park, S.S. (2019). NADPH Oxidase 4 Contributes to Myoblast Fusion and Skeletal Muscle Regeneration. Oxid. Med. Cell. Longev. *2019*, 3585390. https://doi.org/10.1155/2019/3585390.

Yu, M., Wang, H., Xu, Y., Yu, D., Li, D., Liu, X., and Du, W. (2015). Insulin-like growth factor-1 (IGF-1) promotes myoblast proliferation and skeletal muscle growth of embryonic chickens via the PI3K/Akt signalling pathway. Cell Biol. Int. *39*, 910–922. https://doi.org/10.1002/cbin.10466.

Zhang, W., Sun, W., Gu, X., Miao, C., Feng, L., Shen, Q., Liu, X., and Zhang, X. (2022). GDF-15 in tumor-derived exosomes promotes muscle atrophy via Bcl-2/caspase-3 pathway. Cell Death Discov *8*, 162. https://doi.org/10.1038/s41420-022-00972-z.

Stem Cell Reports, Volume *19*

Supplemental Information

Skeletal muscle-on-a-chip in microgravity as a platform for regeneration modeling and drug screening

Soochi Kim, Bugra Ayan, Mahdis Shayan, Thomas A. Rando, and Ngan F. Huang

Supplementary Information:

Skeletal Muscle-On-A-Chip in Microgravity As a Platform for Regeneration Modeling and Drug Screening

Kim *et al.*

Corresponding Authors' Emails: ngantina@stanford.edu and TRando@mednet.ucla.edu

This PDF file includes:

Figures S1 to S5
Tables S1 and S3
Supplementary Tables Legend
Supplementary Experimental Procedures

Other Supplementary Materials for this manuscript include the following:
Tables S2, S4, and S5

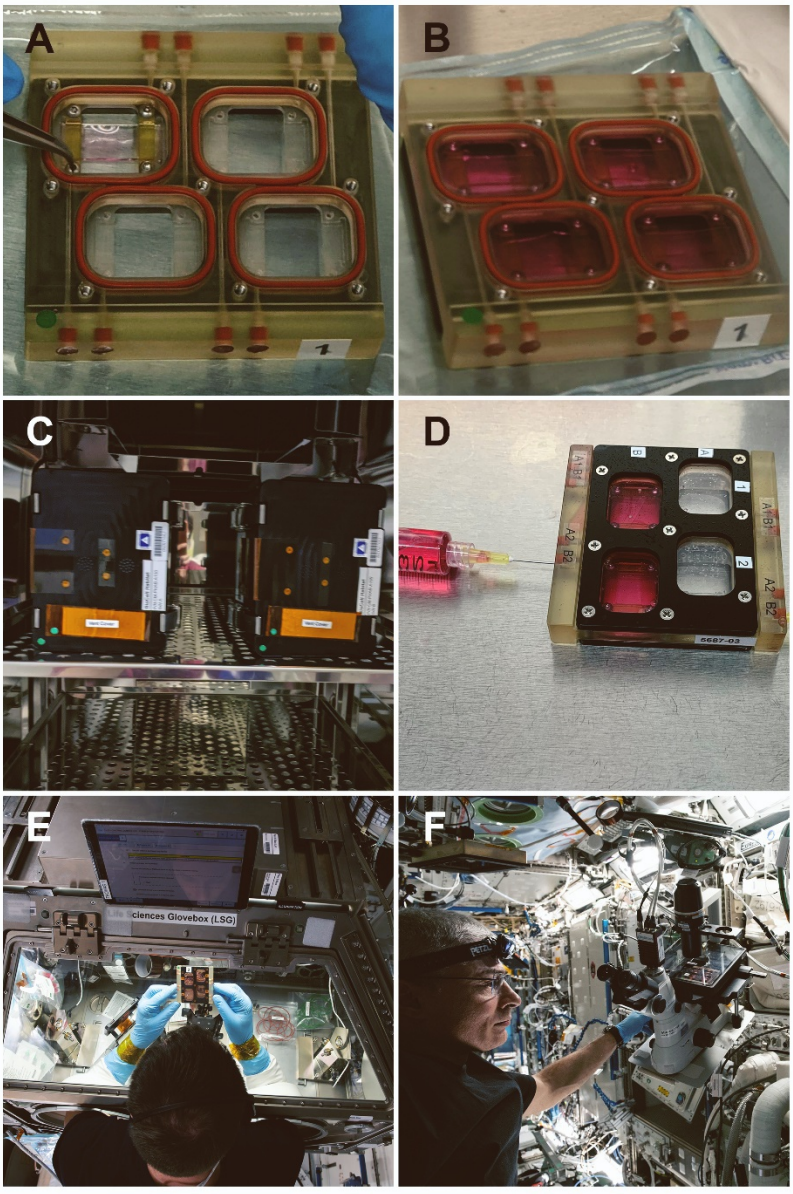

Figure S1. Customized bioreactors for muscle-on-a-chip platform in microgravity, related to Figure 2. A. BioCell bioreactor that houses engineered muscle-on-a-chip. The chips are secured to the bioreactor using screws. **B.** The bioreactor is then filled with media. **C.** Bioreactors are housed within plate habitats that provide temperature maintenance during launch and in microgravity. **D.** Media is changed in microgravity using syringes that exchange media through ports in the bioreactor. **E.** Media exchange is performed in a life sciences glovebox. **F.** Astronauts look at engineered muscle-on-a-chip bioconstructs under a microscope.

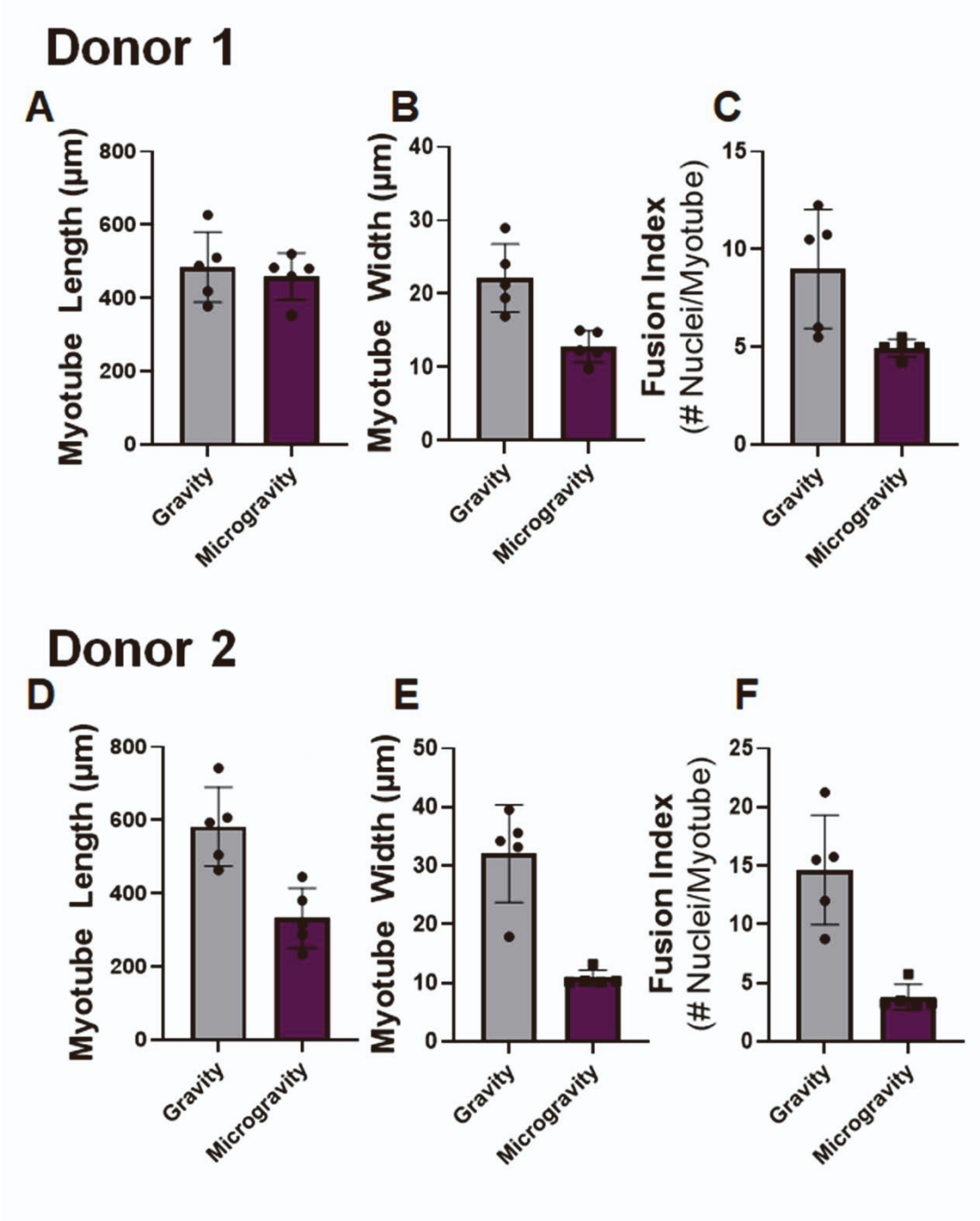

Figure S2. Quantification of myotube formation in muscle-on-a-chip bioconstructs in microgravity, related to Figure 3. A, D. Myotube length quantification in muscle-on-a-chip bioconstructs derived from donors 1 and 2. **B, E.** Myotube width quantification derived from donors 1 and 2. **C, F.** Fusion index quantification in donors 1 and 2. For each of two donor muscle-on-a-chip bioconstructs, 5 confocal images were analyzed and averaged out of 5 images per group. Data is shown as mean ± standard deviation.

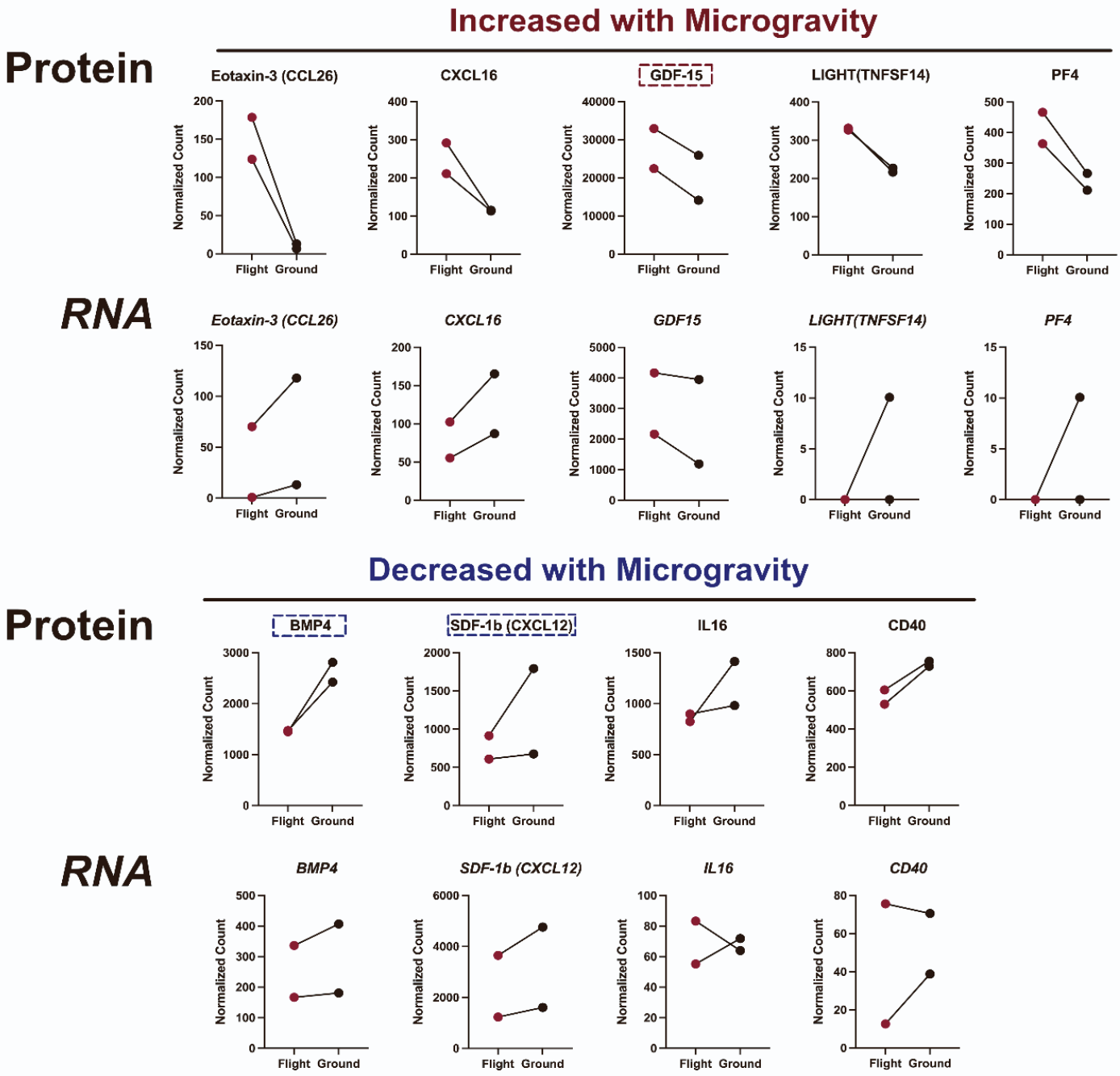

Figure S3. Protein and RNA differences in biomimetic skeletal muscle bioconstructs in microgravity, compared to gravity conditions, related to Figure 3. Symbol and line plots showing differentially expressed proteins in microgravity versus gravity biomimetic skeletal muscle conditioned media and their corresponding RNA levels from bulk RNA seq. Microgravity (flight) or gravity (ground) conditions are denoted, in which lines are associated with the same donor samples. The proteins and corresponding RNA samples and show similar expression level changes are highlighted a dotted box. The data is derived from two donor-derived muscle-on-a-chip bioconstructs per condition.

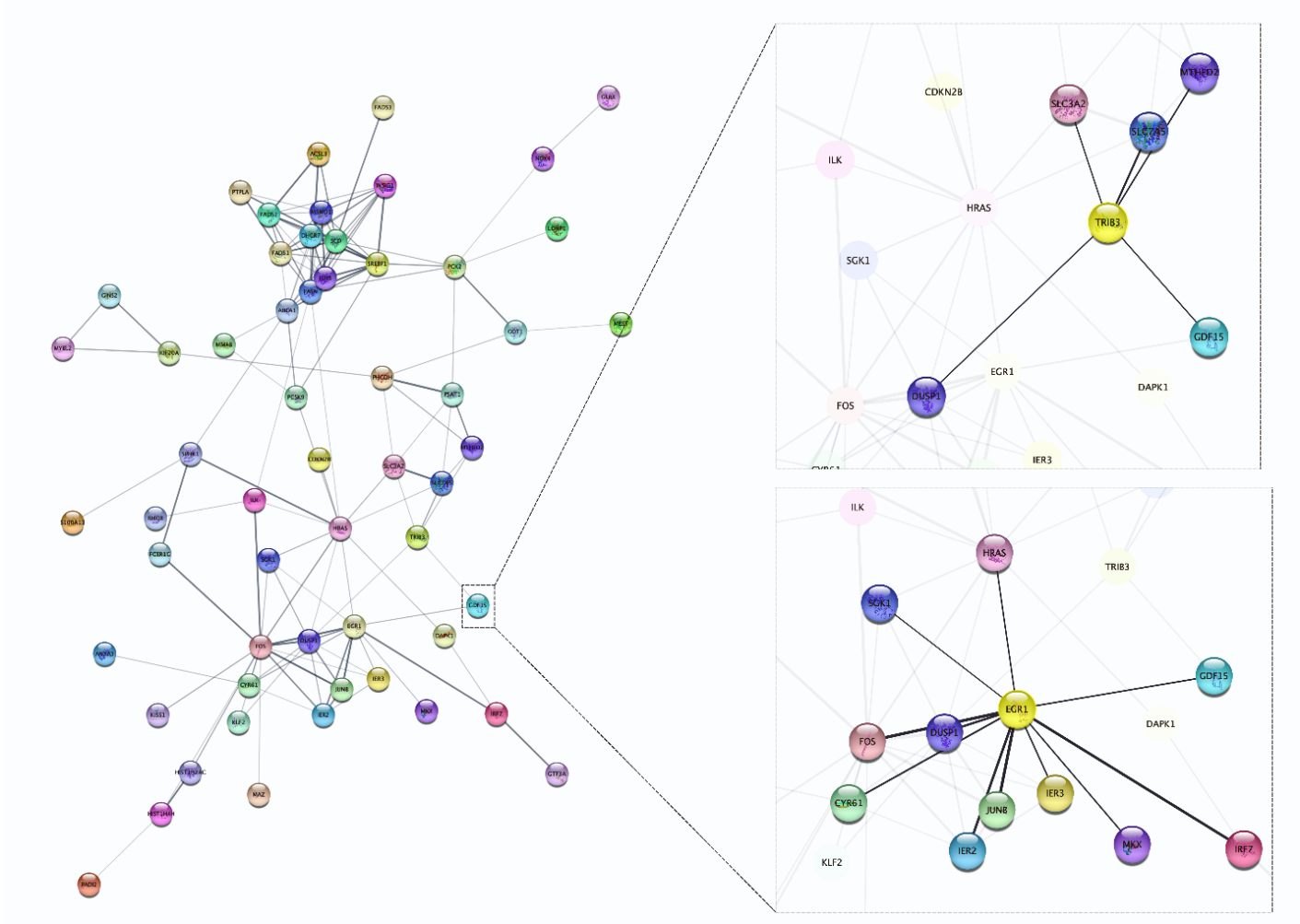

Figure S4. PPI network in space flight biomimetic skeletal muscle, related to Figure 3. The inset highlights GDF-15 and an immediate protein interacting with GDF-15 magnified on the right.

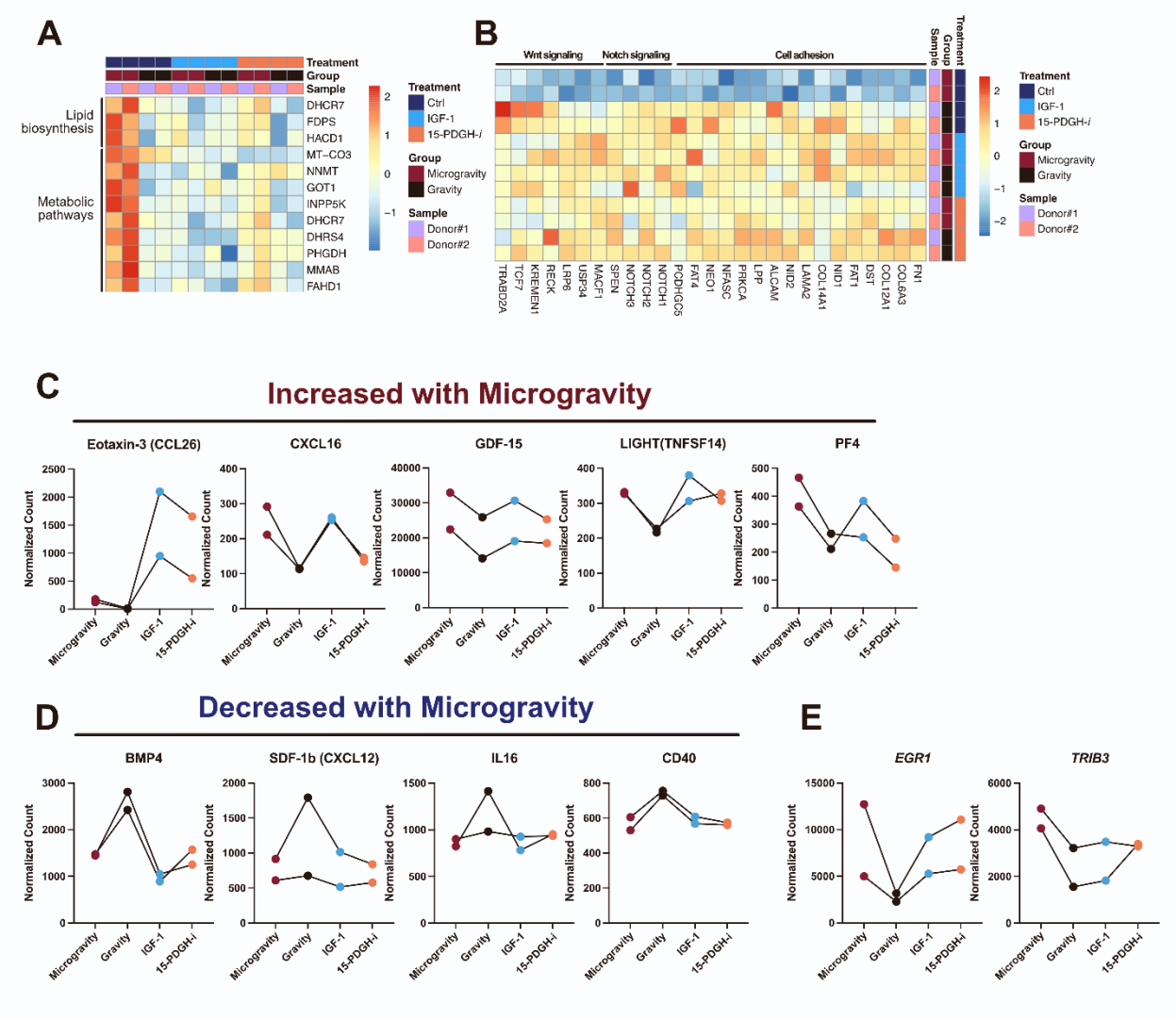

Figure S5. IGF-1 and 15-PDGFH inhibitor (15-PDGH-*i*) treatment partially prevents microgravity effect, related to Figure 5. A. Heatmap showing genes implicated in lipid biosynthesis, metabolic pathways and adipogenesis. **B.** Heatmap showing genes implicated in cell adhesion, Notch signaling and Wnt signaling (n=2 donors per group). Proteins and RNAs whose differential expression could be prevented by IGF-1 or 15-PDGH-*i* treatment (**C-E**). **C-D.** Symbol and line plots showing proteins differentially expressed with microgravity and their levels in biomimetic skeletal muscle conditioned media with drug treatment (IGF-1 or 15-PDGH-*i*). **E.** Symbol and line plots showing EGR1 and TRIB3 RNA levels in microgravity, gravity and drug treated samples. Symbols are colored by microgravity, gravity and drug treated conditions, in which lines join the same donor samples. The data is derived from two donor-derived muscle-on-a-chip bioconstructs per condition.

SUPPLEMENTARY TABLES

Table S1. Quantification of myotube formation in muscle-on-a-chip bioconstructs in microgravity based on myosin heavy chain staining for myotubes, related to Figure 3.

Myotube Length (μm)				**Myotube Width (μm)**				**# Nuclei Per Myotube**			
Donor 1		**Donor 2**		**Donor 1**		**Donor 2**		**Donor 1**		**Donor 2**	
μG	**1G**	**μG**	**1G**	**μG**	**1G**	**μG**	**1G**	**μG**	**1G**	**μG**	**1G**
352	488	315	742	15	17	10	40	5	12	3	21
483	510	445	594	15	19	13	34	4	11	6	12
459	627	287	464	12	21	10	18	6	11	4	9
521	419	234	607	12	29	10	36	5	6	3	16
480	377	380	505	10	24	10	33	5	6	3	16

Abbreviations: Microgravity (μG), Gravity (1G)

Table S3. Demographics of total RNA samples obtained clinical sarcopenia or healthy muscle tissue donors, related to Figure 4.

Sample ID	Age (yr)	Sex	RSM index	Health Status
1	69	Female	4.65	Sarcopenia
2	73	Female	4.96	Sarcopenia
3	48	Female	6.85	Healthy
4	50	Female	7.18	Healthy
5	75	Male	6.26	Sarcopenia
6	64	Male	6.49	Sarcopenia
7	71	Male	7.88	Healthy
8	54	Male	9.82	Healthy

SUPPLEMENTARY TABLE LEGEND

Table S1. Quantification of myotube formation in muscle-on-a-chip bioconstructs in microgravity based on myosin heavy chain staining for myotubes, related to Figure 3.

Table S2. Differentially expressed genes list from microgravity vs gravity samples with log2-fold gene expression levels, related to Figure 3 (n=2 donors per group).

Table S3. Demographics of total RNA samples obtained clinical sarcopenia or healthy muscle tissue donors, related to Figure 4.

Table S4. Differentially expressed genes list from human sarcopenia vs healthy vastus lateralis muscle samples with log2-fold gene expression levels, related to Figure 4 (n=4 donors per group).

Table S5. Proteomic analysis of engineered muscles with drug stimulation in microgravity for 7 days, related to Figure 5.

SUPPLEMENTARY EXPERIMENTAL PROCEDURES

Cell Culture

Primary human skeletal muscle cells (Cell Applications) from two individual donors (37-41 years old) were expanded in growth media consisting of Dulbecco's modified Eagle's medium (DMEM) containing 20% fetal bovine serum (FBS) and 1% penicillin/streptomycin at 37°C and 5% CO_2. The primary cells were used within one passage of thawing.

Fabrication of Aligned Nanofibrillar Collagen Strips

Preparation of the parallel-aligned collagen scaffold was prepared using a shear-based extrusion method, as described in our previous publications (**Figure 1A**) (Alcazar et al., 2020; Hu et al., 2022; Nakayama et al., 2018; Nakayama et al., 2019; Nakayama et al., 2016). Briefly, rat-tail monomeric collagen type I (10 mg/ml in 0.02 N in acetic acid, pH 3.5, Corning) was dialyzed using polyethylene glycol (PEG, Sigma) flakes. Every 15 minutes, the moistened PEG flakes from the surface of the dialysis tubing were removed and replaced with dry PEG flakes and then returned to 4˚C. After 30 minutes, the tubing was placed in a container with MilliQ water, and the moistened PEG was removed from the tubing surface. The dialyzed collagen was spun down at 3000rpm for 1 min to remove air bubbles. Meanwhile, glass slides were submerged inside a Petri dish at 37 °C containing PBS (10X, pH 7.4). Dialyzed monomeric collagen was loaded into a 1-ml syringe with a 22G blunt needle. Thin strips of collagen were extruded onto the glass slides using a steady sideways motion (**Figure 1A**). Extrusion directly into a pH neutral buffer induced fibrillogenesis of the collagen fibrils along the direction of extrusion (**Figure 1B**). The collagen strips were carefully removed from the glass slide, and then 8 strips were adhered as a bundle onto a hydrophobic glass chip (~25x15mm, Schott H, Nexterion). The collagen strips on the glass chips were dried for 2 hours at room temperature until salt crystals started to cover 50%-90% of the surface area. Subsequently, the scaffolds were washed with PBS (1X) and then dried for 24 hours before use. Routine scanning electron microscopy was performed based on previous studies (Huang et al., 2013).

Generation of Muscle-on-a-Chip Bioconstructs and Assembly of Bioreactor

The parallel-aligned nanofibrillar collagen scaffolds immobilized on glass chips were disinfected by soaking in 70% ethanol for 10 minutes, air dried, and then rinsed in PBS (1X) three times before placing into a 6-well plate. Primary human skeletal muscle cells (~$2x10^5$ cells, Cell Applications) from two donors were seeded onto each glass chip and incubated for 24 hours in growth medium. The cell-seeded glass chip is denoted as a 'muscle-on-a-chip'. The muscle-on-a-chip from each donor was transferred to one chamber of a custom-built 4-chamber bioreactor (BioCell, Bioserve Space Technologies) and filled with growth media (**Figure 2A, Figures S1A** and **S1B**). Each tissue chip was immobilized to the bottom of the bioreactor using a stabilizing bridge and overlayed with medium (**Figure S1A**). Once tissue chips were in place, the bioreactor assembly was completed using a transparent oxygen-permeable fluorinated ethylene propylene and bioreactor lid, removing air bubbles and rendering a sealed environment.

Flight Experiment in Microgravity

During transit to the International Space Station National Laboratories (ISSNL) on the NASA Commercial Resupply Mission (NG-16) Cygnus spacecraft, the bioreactors containing muscle-on-a-chip bioconstructs were housed inside space habitats (**Figure 2B, Figure S1C**) that

maintained ~37°C and 5% CO_2 for 7 days without changing their medium. After docking to the ISSNL, the bioreactors were transferred by space astronauts (or flight crew) to the Space Automated Bioproduct Lab for active maintenance of 37°C and 5% CO_2 conditions. The media was exchanged in each chamber by needle/syringe access through designated inset and outlet ports in the bioreactor (**Figure S1D**) in the controlled environment of the life sciences glovebox (**Figure S1E**).

Immunofluorescence Staining of Myotube Formation

Immunofluorescence staining was carried out on fixed cells by permeabilization on 0.1% Triton-X-100, followed by blocking in 1% bovine serum albumin (BSA, Sigma). The primary antibody consisted of skeletal muscle myosin heavy chain (Sigma) at 4°C for 16 hours, followed by incubation in Alexafluor-488-conjugated or Alexafluor-594-conjugated secondary antibody (Fisher Scientific). Total nuclei were visualized by Hoechst 33342 dye (Fisher Scientific). Images of myotube formation in C2C12 myoblasts were acquired using a fluorescence microscope using 10X objectives (BZ-X710, Keyence). For quantification of primary human myotube formation within the bioconstructs after 7 days in microgravity or gravity conditions, images were acquired by confocal microscopy using 10x objectives (Zeiss, LSM-710). In particular, five z-stacks were acquired for each donor engineered muscle sample, and the maximum projection images were taken. Myotube lengths and widths in each image were quantified by ImageJ software. The fusion index was quantified based on the average number of nuclei per myotube.

Sarcopenia Clinical Samples

As a basis for comparison, we further compared the transcriptomes of microgravity samples to that of banked human vastus lateralis muscle total RNA samples. Total RNA from 4 healthy and 4 sarcopenia donors (2 males and 2 females per group) were obtained from University of Kentucky Center for Muscle Biology (**Table S3**) with approval from the Institutional Review Board (Protocol# 46746). Samples were considered to have sarcopenia based on cutoffs for the relative skeletal muscle (RSM) index, which is defined as muscle mass normalized to stature squared (kg/m^2) (Baumgartner et al., 1998). Females with RSM < 5.46 kg/m^2 were considered to have sarcopenia, whereas RSM > 5.46 kg/m^2 were considered to be healthy (Baumgartner, 2000; Kyle et al., 2001). Males with RSM <7.26 kg/m^2 were considered to have sarcopenia, whereas males with RSM > 7.26 kg/m^2 were considered to be healthy (Baumgartner, 2000; Kyle *et al.*, 2001).

Bulk RNA Sequencing and Analysis

Upon sample return to Earth, the muscle-on-a-chip bioconstructs that had been stabilized in RNA Later were dissociated using TrypLE enzyme (Fisher Scientific) for total RNA and total DNA isolation (All Prep Mini Kit, Qiagen). Total RNA samples showing good RNA integrity by Agilent Bioanalyzer analysis were processed for library preparation and bulk RNA Sequencing by Novogene Corporation. In brief, mRNA was purified from total RNA using poly-T oligo-attached magnetic beads. After fragmentation, the first strand cDNA was synthesized using random hexamer primers, followed by the second strand cDNA synthesis. Non-directional library preparation was completed after end repair, A-tailing, adapter ligation, size selection, amplification, and purification. The library was validated using Qubit assay (Fisher Scientific) and quantitative PCR, along with Agilent bioanalyzer analysis of size

distribution detection. The libraries were pooled and sequenced using an Illumina NovaSeq 6000 S4 platform. The paired-end reads were then generated.

The raw data were processed as follows. Raw reads were pre-processed to remove reads containing adapter, poly-N and low-quality reads. Trimmed reads were aligned to the human reference genome (hg38) using Hisat2 (v2.0.5) and featureCounts v1.5.0-p3 was used to generate count reads mapped to each gene. All the downstream analyses were performed on the clean data with high quality, using RStudio software v4.0.4. DESeq2 package v1.30.1 was used for differential gene expression analysis. Statistical analysis was performed using the Wald test statistic, and the resulting p values were adjusted using the Benjaminin and Hochberg's approach for controlling the false discovery rate (FDR). We analyzed microgravity versus gravity (control) bulk RNA sequencing transcriptomics at FDR < 0.1 and sarcopenia versus normal at FDR < 0.25 to assign genes as differentially expressed between the two groups. The raw data files can be accessed from the Gene Expression Omnibus repository (GSE238215).

Gene Ontology (GO) enrichment and pathway enrichment analysis of significantly differentially expressed genes was performed using DAVID (https://david.ncifcrf.gov/) with default settings. We used $P < 0.05$ as significant GO and pathway enrichment.

Custom GSEA Analysis

We computed custom GSEA results for sarcopenia and aging using GSEAplot package v0.1.0 (https://github.com/kelsiereinaltt/GSEAplot) with default settings. In brief, to assess the enrichment of genes associated with sarcopenia or old muscle stem cells, we generated the differentially expressed genes comparing sarcopenia versus normal human muscle tissue. Similarly, we generated differentially expressed genes from a published dataset comparing in vitro cultured old versus young muscle stem cells (Old_MuSC; GSE52699). The expression data were created using create_geneset_db function, which converted the gene list into a novel geneset library, compatible with the GSEAplots function. Finally, our custom geneset libraries (Old_MuSC_UP, Sarcopenia_UP and Sarcopenia_DOWN) were used to compute GSEA analysis on microgravity versus gravity samples.

Proteomics Analysis

The conditioned media collected on day 7 of microgravity were analyzed by the Human Cytokine Array (GS4000, Raybiotech), which utilizes a matched pair of cytokine-specific antibodies for detection for each donor. The arrays were performed by RayBiotech per the manufacturer's instructions. The array consists of 200 cytokines, growth factors, proteases, soluble receptors and other proteins. The protein levels were normalized by DNA concentration and the DESEq2 package v1.30.1 was used for differential protein expression analysis. Statistical analysis was performed using the Wald test statistic, and the resulting p values were adjusted using the Benjaminin and Hochberg's approach for controlling the FDR < 0.25 (n=2 donors per group).

Protein-Protein Interaction Analysis

Protein-protein interaction (PPI) analysis of differentially expressed genes was based on the STRING database (https://string-db.org/). In brief, we retrieved a network for the list of proteins of interest using the multiple proteins search interface, specifying *Homo sapiens* in the Organisms field with default settings.

Drug Screening in Microgravity

As proof of concept for using muscle-on-a-chip bioconstructs for drug screening, two drugs were assessed in microgravity conditions. The first was insulin-like growth factor-1 (IGF-1, 100 ng/ml, Peprotech), which is known to induce proliferation, growth, and regeneration (Alcazar *et al.*, 2020; Ma et al., 2009; Machida and Booth, 2004; Yu et al., 2015). The second was SW033291 (200 nM, Cayman), a small molecule inhibitor of 15-hydroxyprostaglandin dehydrogenase (15-PGDH-*i*) that was previously shown to enhance myogenesis in previous studies (Ho et al., 2017). The drugs were diluted in induction media and loaded into syringes for media exchange on days 0 and 3 in separate bioreactors. On day 7, the conditioned media within the bioreactors were harvested at stored at -80°C. The muscle-on-a-chip bioconstructs within each chamber were treated with RNA Later stabilization agent at stored at -80°C. Upon sample return to Earth about two months later, the bioreactors were processed for RNA Sequencing and proteomics.

SUPPLEMENTARY REFERENCES

Alcazar, C.A., Hu, C., Rando, T.A., Huang, N.F., and Nakayama, K.H. (2020). Transplantation of insulin-like growth factor-1 laden scaffolds combined with exercise promotes neuroregeneration and angiogenesis in a preclinical muscle injury model. Biomater Sci *8*, 5376-5389. 10.1039/d0bm00990c.

Baumgartner, R.N. (2000). Body composition in healthy aging. Ann. N. Y. Acad. Sci. *904*, 437-448. 10.1111/j.1749-6632.2000.tb06498.x.

Baumgartner, R.N., Koehler, K.M., Gallagher, D., Romero, L., Heymsfield, S.B., Ross, R.R., Garry, P.J., and Lindeman, R.D. (1998). Epidemiology of sarcopenia among the elderly in New Mexico. Am. J. Epidemiol. *147*, 755-763. 10.1093/oxfordjournals.aje.a009520.

Ho, A.T.V., Palla, A.R., Blake, M.R., Yucel, N.D., Wang, Y.X., Magnusson, K.E.G., Holbrook, C.A., Kraft, P.E., Delp, S.L., and Blau, H.M. (2017). Prostaglandin E2 is essential for efficacious skeletal muscle stem-cell function, augmenting regeneration and strength. Proc. Natl. Acad. Sci. U. S. A. *114*, 6675-6684. 10.1073/pnas.1705420114.

Hu, C., Ayan, B., Chiang, G., Chan, A.H.P., Rando, T.A., and Huang, N.F. (2022). Comparative Effects of Basic Fibroblast Growth Factor Delivery or Voluntary Exercise on Muscle Regeneration after Volumetric Muscle Loss. Bioengineering (Basel) *9*, 37. 10.3390/bioengineering9010037.

Huang, N.F., Okogbaa, J., Lee, J.C., Jha, A., Zaitseva, T.S., Paukshto, M.V., Sun, J.S., Punjya, N., Fuller, G.G., and Cooke, J.P. (2013). The modulation of endothelial cell morphology, function, and survival using anisotropic nanofibrillar collagen scaffolds. Biomaterials *34*, 4038-4047. 10.1016/j.biomaterials.2013.02.036.

Kyle, U.G., Genton, L., Hans, D., Karsegard, V.L., Michel, J.P., Slosman, D.O., and Pichard, C. (2001). Total body mass, fat mass, fat-free mass, and skeletal muscle in older people: cross-sectional differences in 60-year-old persons. J. Am. Geriatr. Soc. *49*, 1633-1640. 10.1046/j.1532-5415.2001.t01-1-49272.x.

Ma, Q.L., Yang, T.L., Yin, J.Y., Peng, Z.Y., Yu, M., Liu, Z.Q., and Chen, F.P. (2009). Role of insulin-like growth factor-1 (IGF-1) in regulating cell cycle progression. Biochem. Biophys. Res. Commun. *389*, 150-155. 10.1016/j.bbrc.2009.08.114.

Machida, S., and Booth, F.W. (2004). Insulin-like growth factor 1 and muscle growth: implication for satellite cell proliferation. Proc. Nutr. Soc. *63*, 337-340. 10.1079/PNS2004354.

Nakayama, K.H., Alcazar, C., Yang, G., Quarta, M., Paine, P., Doan, L., Davies, A., Rando, T.A., and Huang, N.F. (2018). Rehabilitative exercise and spatially patterned nanofibrillar scaffolds enhance vascularization and innervation following volumetric muscle loss. Npj Regen Med *3*, 16. 10.1038/s41536-018-0054-3.

Nakayama, K.H., Quarta, M., Paine, P., Alcazar, C., Karakikes, I., Garcia, V., Abilez, O.J., Calvo, N.S., Simmons, C.S., Rando, T.A., and Huang, N.F. (2019). Treatment of volumetric muscle loss in mice using nanofibrillar scaffolds enhances vascular organization and integration. Communications biology *2*, 170. 10.1038/s42003-019-0416-4.

Nakayama, K.H., Surya, V.N., Gole, M., Walker, T.W., Yang, W., Lai, E.S., Ostrowski, M.A., Fuller, G.G., Dunn, A.R., and Huang, N.F. (2016). Nanoscale Patterning of Extracellular Matrix Alters Endothelial Function under Shear Stress. Nano Lett *16*, 410-419. 10.1021/acs.nanolett.5b04028.

Yu, M., Wang, H., Xu, Y., Yu, D., Li, D., Liu, X., and Du, W. (2015). Insulin-like growth factor-1 (IGF-1) promotes myoblast proliferation and skeletal muscle growth of embryonic chickens via the PI3K/Akt signalling pathway. Cell Biol. Int. *39*, 910-922. 10.1002/cbin.10466.